Development and Characterization of Gas Diffusion Layer Using Carbon Slurry Dispersed by Ammonium Lauryl Sulfate for Proton Exchange Member Fuel Cells

by

Rashida Villacorta

A Thesis Presented in Partial Fulfillment
of the Requirements for the Degree
Master of Science in Technology

Approved June 2012 by the
Graduate Supervisory Committee:

Arunachalanadar Madakannan, Chair
Xihong Peng
Govindasamy Tamizhmani

ARIZONA STATE UNIVERSITY

August 2012

ABSTRACT

Gas diffusion layers (GDLs) are a critical and essential part of proton exchange membrane fuel cells (PEMFCs). They carry out various important functions such as transportation of reactants to and from the reaction sites. The material properties and structural characteristics of the substrate and the microporous layer strongly influence fuel cell performance. The microporous layer of the GDLs was fabricated with the carbon slurry dispersed in water containing ammonium lauryl sulfate (ALS) using the wire rod coating method. GDLs were fabricated with different materials to compose the microporous layer and evaluated the effects on PEMFC power output performance. The consistency of the carbon slurry was achieved by adding 25 wt. % of PTFE, a binding agent with a 75:25 ratio of carbon (Pureblack and vapor grown carbon fiber). The GDLs were investigated in PEMFC under various relative humidity (RH) conditions using H_2/O_2 and H_2/Air.

GDLs were also fabricated with the carbon slurry dispersed in water containing sodium dodecyl sulfate (SDS) and multiwalled carbon nanotubes (MWCNTs) with isopropyl alcohol (IPA) based for fuel cell performance comparison. MWCNTs and SDS exhibits the highest performance at 60% and 70% RH with a peak power density of 1100 $mW.cm^{-2}$ and 850 $mW.cm^{-2}$ using air and oxygen as an oxidant. This means that the gas diffusion characteristics of these two samples were optimum at 60 and 70 % RH with high limiting current density range. It was also found that the composition of the carbon slurry, specifically ALS concentration has the highest peak power density of 1300 and

500mW.cm^{-2} for both H_2/O_2 and H_2/Air at 100% RH. However, SDS and MWCNTs demonstrates the lowest power density using air and oxygen as an oxidants at 100% RH.

DEDICATION

To my mother, Ludivina Ferrer Villacorta,

for her perpetual love, encouragement, and support.

ACKNOWLEDGMENTS

First and foremost, I would like to grant my sincere gratitude to my advisor and committee chair, Dr. Arunachalanadar Madakannan, for providing me with his unsurpassed support, guidance and wisdom throughout my graduate studies. I cannot express enough of my appreciation for inspiring and developing my interest to become successful and dedicated in this field and as a student.

I wish to express my thanks to my academic committee members, Dr. Govindasamy Tamizhmani Xihong Pheng for their interest, time, valuable contribution and guidance throughout this thesis work.

I want to greatly acknowledge I would like to thank my colleagues and friends, Anthony Adame, Jameel Armstrong, Xuan Liu, Kartik Kinhal, Qurat-ul-ain Shah, Yen Huang, Adam Arvay, Chad Mason, Brian Fauss, and Aditi Jhalani for their support and encouragement throughout my thesis work.

I would also like to extent my gratitude to Jay Lin, whose contributions to Fuel Cell Laboratory are invaluable. His guidance and support for his colleague to become successful is beyond words.

I would like to acknowledge and thank Mr. Rene Fischer for his assistance and support in fixing and troubleshooting the equipments in Fuel Cell Lab. I would also like to thank Ms. Cheryl Roberts for her assistance in ordering supplies, Julie Barnes and Martha Benton for their support during the course of my graduate study and thesis work.

I would like to thank ASU/NASA Space Grant Program, Dr. Thomas Sharp and Candace Jackson for their support during my time as a Space Grant Intern which led to this research work.

I would like to express my sincerely appreciation to Sally Villacorta for her encouragement and continued support for my education and well being. I would also like thank my family and friends for their kind words of encouragement and support.

My deepest gratitude for my mother for her precious love and support. Thank you for all your sacrifices and teaching me the value and importance of education. You are the reason I am here, and made me who I am today. And to my fiancé, Robert Edward Gordon, who is my inspiration in everything I do and every choices I make. He also inspires me to be a better person every day, encourages me to pursue all of my dreams, and has the patience and endurance to stand by me. I thank God for blessing me with your love and for coming into my life.

TABLE OF CONTENTS

Page

LIST OF TABLES viii

LIST OF FIGURES ix

CHAPTER

1 INTRODUCTION 1

Background 1

Statemen of Problem 7

Scope of Work 8

Organization of the Thesis 9

2 LITERATURE REVIEW 11

2.1 Historical Highlights 11

2.2 Proton Exchange Membrane (PEMFC) 13

2.2.1 Efficiency, Power and Energy on PEMFC 14

2.2.2 Operational Losses in PEMFC 16

2.3 Technical Challenges of PEMFC applications 19

2.4 GDLs 24

2.5 Surfactant Materials for GDLs 25

2.6 GDLs Characterization Techniques 30

2.6.1 Electrochemical Impedance Spectroscopy 31

3 EXPERIMENTAL 34

3.1 Gas diffusion Layer 34

3.1.1 Fabrication process of ALS based GDL 34

CHAPTER Page

3.1.2 Fabrication process of MWCNTs with ALS based GDL 36

3.1.3 Fabrication process of SDS based GDL 36

3.2 Catalyst 39

3.3 Membrane Electrode Assembly and Fuel Cell Performance 40

3.4 Optimizing GDLs Properties 42

4 RESULTS AND DISCUSSION 43

4.1 Fuel Cell Performance 44

4.2 EIS Analysis 49

5 CONCLUSION 57

REFERENCES 60

LIST OF TABLES

Table Page

1. Typical characteristics of different types of fuel cells 4

2. GDL samples was fabricated with different ALS concentration 37

3. Composition of SDS and ALS for comparison and evaluation..... 37

4. Fuel cell performance summary of ALS, MWCNTs and SDS 49

LIST OF FIGURES

Figure Page

1. Figure 1 Schematic diagram of PEMFC 6
2. Figure 2 Hydrogen fuel cell or gaseous voltaic battery 11
3. Figure 3 Graph of voltage vs. current density of H_2/Air PEMFC 14
4. Figure 4 Ideal and actual fuel cell voltage/current characteristics..... 16
5. Figure 5 Tafel plots for slow and fast electrochemical reactions 17
6. Figure 6 PEM fuel cell stack cost components 19
7. Figure 7 Platinum prices 20
8. Figure 8 Self-assembled monolayer structure of SDS micelles on MWCNTs..... 25
9. Figure 9 Ammonium lauryl sulfate chemical structure 26
10. Figure 10 The icosahedral C60 molecule..... 27
11. Figure 11 Multiwalled carbon nanotubes..... 28
12. Figure 12 Equivalent circuit element for a single cell fuel cell 33
13. Figure 13 Fabrication process of ALS based GDL..... 35
14. Figure 14 Fabrication process of MWCNTs based GDL 36
15. Figure 15 Fabrication process of SDS based GDL 36
16. Figure 16 Easycoate equipment (EC26 Coatema) 38
17. Figure 17 Schematice representation of micelle-encapsulated Pureblack and VGCF..... 38
18. Figure 18. a) Homemade fixture for CCM b) CCM micro-spray method..... 39

Figure Page

19. Figure 19 Greenligh test station(G50 Fuel Cell System, Hydrogenics Vancouver, Canada 41

20. Figure 20 Diagram of improving parameters of GDLs 42

21. Figure 21 Fuel cell performance of various ALS concentration at 80^{o}C 44

22. Figure 22 ALS fuel cell performance at different RH conditions using H_2/O_2 45

23. Figure 23 ALS fuel cell performance at different RH conditions using H_2/Air 46

24. Figure 24 MWCNTswith ALS fuel cell performance at different RH conditions using H_2/O_2 conditions 46

25. Figure 25 MWCNTs with ALS fuel cell performance at different RH conditions using H_2/Air conditions 47

26. Figure 26 SDS fuel cell performance at different RH conditions using H_2/O_2 conditions 47

27. Figure 27 SDS fuel cell performance at different RH conditions using H_2/Air conditions 48

28. Figure 28 Fuel cell performance of ALS, MWCNTs and SDS at 100% RH conditions, 80^{o}C using H_2/O_2 conditions 48

29. Figure 29 Electrochemical impedance spectroscopy of MWCNTs with ALS 52

Figure Page

30. Figure 30 Electrochemical impedance spectroscopy of ALS 54

31. Figure 31 Electrochemical impedance spectroscopy of SDS 55

32. Figure 32 Fuel cell performance and electrochemical impedance spectroscopy (EIS) of ALS, MWCNTs with ALS and SDS 56

Chapter 1

INTRODUCTION

The consumption of energy is a fundamental part of today's world. Over the last decade, its usage has drastically increased the quality of life of modern society and has allowed for the rapid advancement of modern technology. The majority of what we consume in our daily activities to power our homes, schools, offices and automobiles requires energy created from fossil fuels. These nonrenewable fuel sources may be easily accessible and generate large amounts of electricity at relatively low cost, but their continued use has resulted in increased health risks, environmental pollution, and global warming. Fortunately, as an alternative to traditional sources of power, fuel cell technology has the potential to meet the energy demands of our growing population and reduce many of the conflicts fossil fuels are causing in an environmentally friendly manner.

Fuel cells share similarities with internal combustion engines and batteries, as they are all electrochemical device converters. Batteries store the chemical reactants of typically metal compounds such as alkaline, lithium, or zinc, and once consumed may be either recharged or disposed. However, internal combustion engines convert chemical to mechanical energy.

Because of their zero emissions, simple design, accessibility, and high efficiency, hydrogen fuel cells present one of the best alternatives to the internal combustion engine. Essentially, a fuel cell generates electricity through reactants (hydrogen and oxygen) that are stored externally and will produce electricity as long as it has a fuel supply. Fuel cells are electrochemical devices that convert

chemical energy directly into electricity and heat with high efficiency. In other words, they are energy conversion devices for power generation that have the capability of producing electrical energy as long as the fuel and oxidant are supplied to the electrodes.

There are both attractive features and challenging limitations to fuel cell technologies [1]. The attractive features that fuel cells offer are:

- The potential for a high operating efficiency.
- A highly scalable design.
- Zero or near-zero greenhouse emissions.
- No moving parts, making them more reliable and quieter than generators
- In comparison to batteries, fuel cells have nearly instantaneous recharge capability.

In order for the fuel cell technologies to be viable for commercialization, there are several limitations that first need to be addressed:

- Fuel cells have to be cost-effective, mass produced pure hydrogen storage and delivery.
- Fuel cells requires pure hydrogen, if not supplied the performance will gradually decreases because of catalyst degradation and electrolyte poisoning.
- Fuel reformation technology can be costly and heavy, requiring power in order to operate.

- Durability issues are one of the constraints in fuel cell technologies.

Fuel cells can be classified according to electrolyte usage. The five most common types of fuel cell technologies are:

- Alkaline fuel cells (AFCs)
- Solid oxide fuel cells (SOFCs)
- Proton exchange membrane fuel cells (PEMFCs)
- Phosphoric acid fuel cells (PAFCs)
- Molten carbonate fuel cells (MCFCs)

As illustrated in the Table 1, different types of fuel cells operates at various temperature ranges from 50 -1000^{o}C and each type of fuel cells uses different electrolytes. The higher energy conversion efficiency is the result of high temperature, for example, AFCs and PEMFCs. Furthermore, the applications of each fuel cell types were illustrated in the table below.

TABLE I

Typical characteristics of different types of fuel cells [2, 3]

Fuel Cell Type	Operating Temperature (^{o}C)	Electrolyte	Typical Stack	Efficiency (%)	Applications
AFCs	50-200	Aqueous solution of potassium hydroxide soaked in a matrix	10kW-1MW	60	Space, military and residential plants
SOFCs	600-1000	Yttria stabi-lized zirconia	<1kW-3MW	60	Auxiliary power and electric utility
PEMFCs	30-100	Solid organic polymer poly-perfluorosul-fonic acid	<1kW-250kW	35-60	Vehicles, portable power, electrical utility
PAFCs	~220	Liquid phosphoric soaked in matrix	50kW-1MW	40	Electric utility and transportation
MCFCs	~650	Solution of lithium, sodium, and potassium carbonates	1kW-1MW	45-50	Electric utility or medium to large scale CHP systems, up to MW capacity

There are several types of fuel cells, but the most popular and research type are proton exchange membrane fuel cells (PEMFCs). Traditionally the PEMFCs uses hydrogen as a fuel. They have relatively low operational temperature, which is under 100 ^{o}C, high power density and efficiency, as well as the ability to respond quickly to transient power. Despite the positive qualities of PEMFCs, cost, reliability and durability remain the major barriers for wide-scale

commercialization. In proton exchange membrane fuel cells, platinum (Pt) is the most effective electrocatalyst because it is sufficiently reactive in bonding hydrogen and oxygen intermediates, facilitating the electrode processes to form the final product. However, the significantly high cost of Pt in practical PEMFCs limits the catalyst loadings per unit area (or unit power output).

The basic physical structure of a PEMFC contains three main components: bipolar plate (gas channel), gas diffusion layer (GDL), and membrane electrode assembly (MEA). The MEA is sandwiched with two GDLs on both sides and the electro-chemical processes are taking place in the interface between MEA and GDLs. The durability of PEMFCs system is typically controlled by the stability of membrane electrode assembly (MEA). The fuel cell consists of an electrolyte layer in contact with a porous anode and cathode on either side. Figure 1 [4] below is an illustration of a fuel cell with reactant/product gases and the ion conduction flow direction through the cell. Hydrogen enters on the anode side (negative electrode) where hydrogen oxidation reactions (HOR) occur. With the help of catalyst, the hydrogen with split into electrons and protons. The electrons are channeled through a circuit and produce electricity, while protons pass through the polymer electrolyte membrane. On the cathode side (positive electrode), oxygen or air enters the assembly, at which point oxygen reduction reactions (ORR) occurs. Oxygen will combine with protons and electrons and form water. Also water vapor and heat are released as byproducts of this reaction.

The chemical reactions in a fuel cell at the electrodes are:

- Anode: H_2 (g) → $2H^+$ (aq) + $2e^-$
- Cathode: ½ O_2 (g) + $2H^+$ (aq) + $2e^-$ → H_2O (l)
- Overall: H_2 + ½O_2 → H_2O + electricity + waste heat

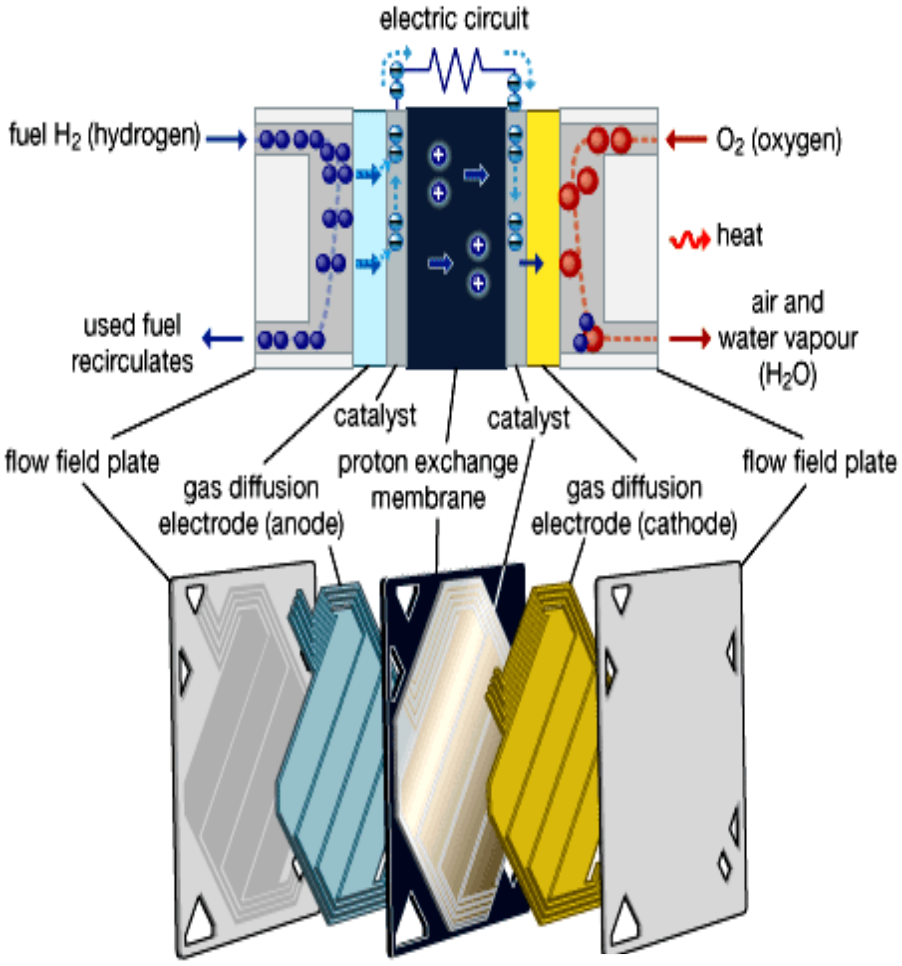

Figure 1. Schematic Diagram of Proton Exchange Membrane Fuel Cell [4]

1.2 Statement of Problem

The PEMFC has the greatest potential as an alternative power source for transportation due to its relatively low temperature of operation (<100^{o}C) and stationary applications. However, in order to be viable for commercialization, PEMFC should overcome the critical challenges related to cost, performance, reliability, and durability. The cost for fuel cell system should be drastically reduced to compete with the internal combustion engine and stationary power generation. According to the U.S. Department of Energy (DOE), in 2002 the cost of automotive fuel cell system was significantly reduced from $ 275/kW to $73/kW in 2008, and $45/kW in 2010. However, the DOE's target is to reduce the cost to $30/kW with 5000 hours (150,000 mile) durability for automotive fuel cell systems by 2015, and for stationary fuel cells is $750/kW with 40,000 hours durability by 2011 [5].

The gas diffusion layer (GDL) is one of the critical components acting both as the functional as well as the support structure for the membrane-electrode assembly in PEMFC [6]. The main function of the GDL is used to effectively transport reactant gases and electrons as well as remove product water and heat. For this reason, the effective functionality of the GDL plays significant role in making the PEMFC commercially viable. The power performance of the PEMFC is strongly influenced by interdependent properties such as water management, porosity and graded structure of the GDL. In order to achieve a high power performance, the GDL should combine and properties of hydrophobicity (water expelling) and hydrophilicity (water retaining). These properties should be

critically examined, and balanced carefully to ensure that the fuel cell system works without flooding, high humidity (100% relative humidity) and drying of the electrolyte at lower relative humidity. The GDLs should exhibit properties such as good diffusion [7, 8] with optimum bending stiffness, porosity, surface contact angle, air permeability, water vapor diffusion, electrical/electronic conductivity, crack free surface morphology, high mechanical integrity and enhanced oxidative stability, along with durability at various operating conditions including freezing [6].

1.3 Scope of Work

The focal point of this research work is primarily on the proton exchange membrane fuel cell. This thesis will entail and achieve the following objectives: a comparison of proton exchange membrane fuel cell (PEMFC) performance when using different materials to compose the microporous layer of the gas diffusion layer (GDL). The comparison is valuable in that using different materials changes the porosity, particle size, and conductivity of the microporous layer, which can affect PEMFCs power output. The experimentation of different materials was conducted using the Fuel Cell Test System and electrochemical impedance spectroscopy (EIS) to determine the effect of these changes on PEMFC performance (power output).

- The comparison and evaluation of sodium dodecyl sulfate (SDS) and ammonium lauryl sulfate (ALS) surfactant, multiwalled carbon nanotubes (MWCNTs) and polytetrafluoroethylene (PTFE), hydrophobic binding agent.

- Fabrication and characterization of GDLs with premium properties for high power PEMFCs.
    a) Optimization of GDL with ALS based compositions
    b) Fabrication of GDL by wire rod coating procedure

1.4 Organization of the Thesis

This thesis is organized to provide an in-depth understanding of the research work accomplished.

1) Chapter One gives an introduction to the thesis including background information and the scope of the proposed work.

2) Chapter Two entails a comprehensive literature review of PEMFC technology: the historical highlights of PEMFC, the technical challenges facing the technology, surfactants materials and fabrication of GDLs, and other valuable research work achieved that are significant to this thesis.

3) Chapter Three describes the experimental procedures and settings to prepare gas diffusion layer. Also, the development and characterization of the different materials for GDLs.

4) Chapter Four discusses the results of this thesis research by implementing various tools such as PEMFC test and electrochemical impedance spectroscopy (EIS) to evaluate the characterization of GDLs.

5) Chapter Five presents the summary and conclusion of the research performed in this thesis. In addition, it also provides the recommendations for future research.

Chapter 2

LITERATURE REVIEW

2.1 Historical Highlights

It may be thought that fuel cells are a modern technology, yet in truth they have existed for over a century. Sir William Grove, the "father of the fuel cell," first developed and demonstrated the concept of the fuel cell in 1839. The diagram below (Fig. 2) is a version of Grove's drawing of the original hydrogen fuel cell, which he called the "Gaseous Voltaic Battery." However, Grove's invention failed to produce enough electricity to be useful. The first working fuel cell was invented by Ludwig Mond and Charles Langer in 1889, where they utilized air and industrial coal gas.

The first proton exchange membrane (PEMFC) was developed in the early 1960s by Thomas Grubb and Leonard Niedrach at General Electric Company ®. The fuel cell was powered by hydrogen generated by mixing water and lithium hydride [2]. The device was compact, and platinum (Pt) was used as the catalyst. Due to the high cost of platinum in the manufacturing of PEMFCs, this technology was primarily used for applications related to the space program. The interest in PEMFCs increased tremendously during 1980s and 1990s. Ballard Power System (founded in 1979) developed and demonstrated the first hydrogen-fueled PEM fuel cell bus, signaling that the applications of PEMFCs could be successfully extended. The development of PEMFC technology has the

significant potential to solve the growing concerns regarding global warming, environmental pollution, depletion of fossil fuels, and the energy demands of our growing population. Governments, industries, and academic institutions all the world have begun serious research into overcoming the obstacles to their widespread commercialization. Most research is dedicated to developing the materials needed, identifying the fuel source, and decreasing the cost of this technology.

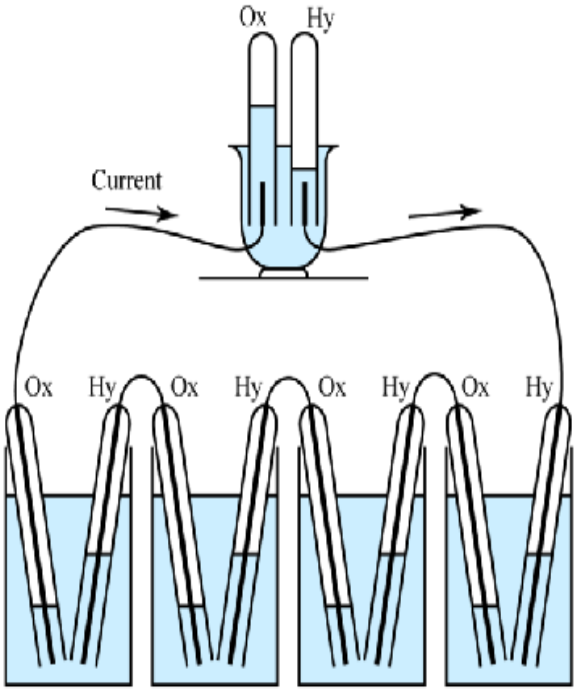

Figure 2. Hydrogen fuel cell or "Gaseous Voltaic Battery"[10]

Furthermore, various state governments are enthusiastically promoting the use of renewable energies. For example, the state of California has several stations for hydrogen powered fuel cell vehicles, which increases their public profile and further validates future research into the technology investigated in

this thesis. Indeed, the state of Arizona also provides various legal and financial incentives promoting broader hydrogen fuel cell utilization, such as tax, parking, and high occupancy vehicle exemptions [7]

2.2 Proton Exchange Membrane Fuel Cell (PEMFC)

In PEMFCs, the chemical reaction is quite simple. Hydrogen molecules split into hydrogen ions and electrons on the anode, while protons recombine with oxygen and electrons into water and release heat on the cathode. On the other hand, a fuel cell can be very complicated and delicate mechanically due to the specific requirements of high power output, which requires fast reaction, durability and economical effectiveness. Figure 1 shows the schematic of a PEMFC together with the electrode reactions. The major elements discussed and showed in figure 1are: a catalyst layer containing platinum and/or platinum alloy which is used to catalyze the electrode reactions, gas diffusion medium that often consist of a microporous layer (MPL) and a carbon fiber based gas diffusion layer (GDL). The GDL is used to effectively transport reactant gases and electrons as well as remove product water and heat, and finally a flow field plate is needed to uniformly distribute the reactant gas.

PEMFC systems are typically evaluated on the basis of their performance vis-à-vis power density, efficiency and durability. However, proper functionality is not easily evaluated or assessed through the narrowly defined performance of the fuel cell electrochemical reactions. All electrochemical processes involve the transfer of electron between an electrode and a chemical species with a change in

Gibbs free energy. [11]. As shown in Figure 1, in the PEMFC the electro-chemical reaction takes place in the interface between the electrode (catalyst layer) and the electrolyte. Each charge should pass through an "activation energy barrier" in order to move through the electrolyte, electrode, or bipolar plate. The dependency of the electrochemical reactions is a result of how fast the electrons are created or consumed. Faraday's Law expresses the rate of charge transfer and how current is a direct measure of the electrochemical reactions.

The equation below states Faraday's Law;

$$i = dQ/dt \qquad \text{Eq. 1}$$

where Q is the charge and t is the time.

2.2.1 Efficiency, Power and Energy on PEMFC

In a hydrogen fuel cell, the energy conversion can be illustrated in the equation below:

Chemical Energy of Fuel = Electric energy + Heat energy

An ideal H_2/Air single cell stack could produce 1.16V when the current is an open circuit voltage (zero), and the temperature is 80 degrees Celsius at one atmospheric pressure gas. A good measure of energy conversion efficiency for a fuel cell is the ratio of the actual cell voltage to the theoretical maximum voltage for the H_2/Air reaction. A fuel cell operating at 0.7 V is generating approximately 60% of the maximum useful energy available from the fuel in the form of electric power. If the same fuel cell is operated at 0.9 V, about 77.5% of the maximum useful energy is being delivered as electricity. The remaining

energy (40% or 22.5%) will appear as heat. The characteristic performance curve for a fuel cell represents the DC voltage delivered at the cell terminals as a function of the current density. In other words, the total current is divided by the area of membrane being drawn from the fuel cell to the load in the external circuit (Fig.3). [12]

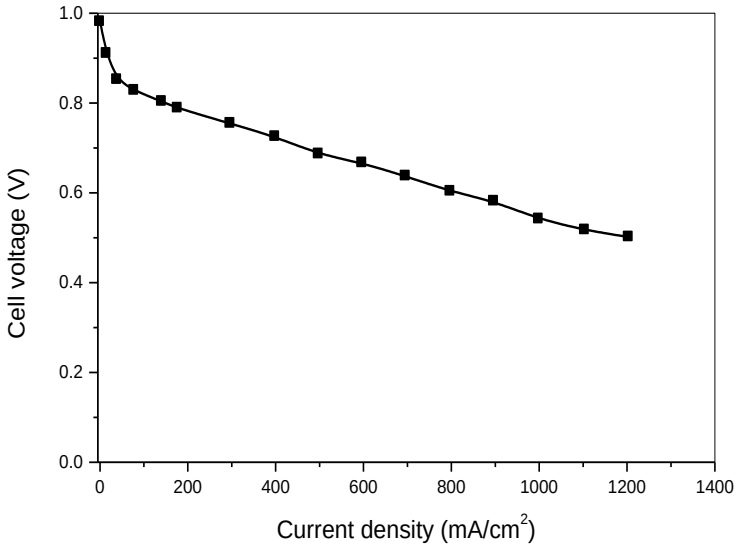

Figure 3. Graph of voltage vs. current density of H_2/Air PEMFC [12]

The power (P), expressed in units of watts, delivered by a cell is the product of the current (I) drawn and the terminal voltage (V) at that current (P = IV). Power is also the rate at which energy (E) is made available (P = E/t) or conversely, energy, expressed in units of watt-hours, is the power available over a period of time (t) (E = Pt). As the mass and volume of a fuel cell system are so important, additional terms are also used. Specific power is the ratio of the power produced by a cell to the mass of the cell; power density is the ratio of the power

produced by a cell to the volume of the cell. High specific power and power density are important for transportation applications to minimize the weight and volume of the fuel cell as well as to minimize cost.

2.2.2 Operational Losses in PEMFC

The actual cell potential is decreased from its equilibrium potential because of irreversible losses as shown in Figure 4 below. The multiple phenomena contribute to irreversible losses in an actual fuel cell. The reversible OCV of a hydrogen fuel cell is given by the equation,

$$E = -\Delta g\, f / zF \qquad \text{Eq. (2)}$$

When a fuel cell operates, the voltage is less than this. The figures show the performance of a typical single cell operating at about 70 ^{o}C, at normal air pressure. The losses which are called polarization, over potential, or over voltage which originate from these three sources:

- Activation Losses
- Ohmic polarization
- Concentration polarization

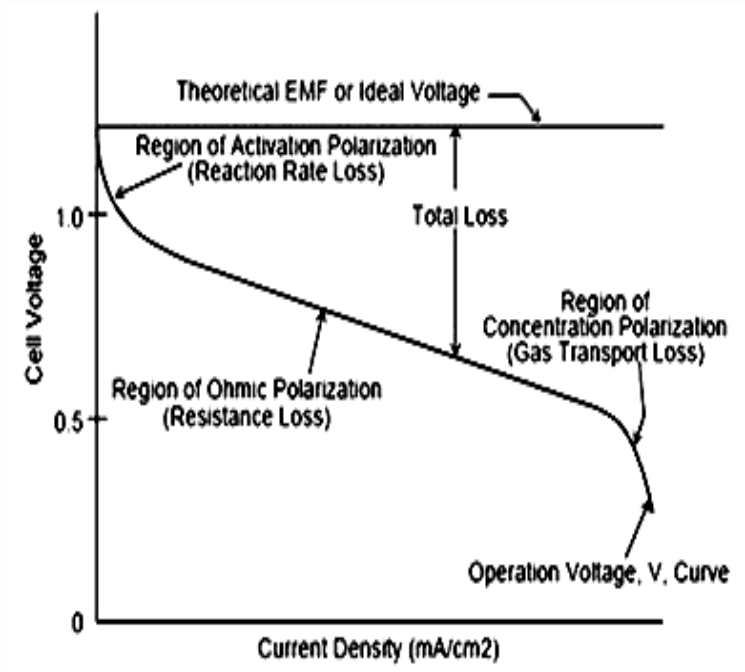

Figure 4. Ideal and Actual Fuel Cell Voltage/Current Characteristic [13]

• Activation Polarization

The activation polarization loss (dominant at low current density) is present when the rate of the electrochemical reaction at the electrode surface is controlled by sluggish electrode kinetics [14]. These are caused by the slowness of the reactions taking place on the surface of the electrode. A proportion of the voltage generated is lost in driving the chemical reaction that transfers the electrons to or from the electrode. Activation losses increase as the current increases. The activation losses can be obtained by Tafel:

$$\Delta V_{act} = A \ln(i / i_o)$$

where A is a constant, V is the overvoltage, i is the current density, and i_0 is the current density at which the overvoltage begins to drop (or from zero). It is

critical to know that Tafel equation is only true when $i > i_{o.}$ The diagram (fig.4) shows the two typical plots.

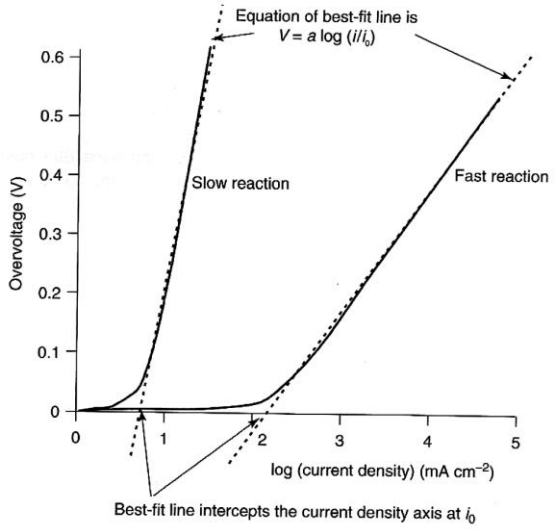

Figure 5. Tafel plots for slow and fast electrochemical reactions [15]

- Ohmic Polarization (Loss)

The ohmic loss is due to the resistance of the polymer electrolyte membrane to the ions and the resistance of imperfect electrodes. The loss (voltage drop) in the fuel cell is approximately linear in this region. The dominant ohmic losses through the electrolyte are reduced by decreasing the electrode separation and enhancing the ionic conductivity of the electrolyte. As the electrolyte and electrodes comply with Ohm's Law, the ohmic losses can be expressed by the equation $E = IR$, where I is current flowing through the cell and R is the total resistance.

• Concentration Polarization (Mass Transportation Losses)

The concentration polarization relates to the change in the concentration of the reactants at the surface of the electrodes as the fuel (hydrogen) is used. The concentrations of the fuel and oxidant are reduced at the various points in the fuel-cell gas channels and are less than the concentrations at the inlet portion of the stack. This loss becomes significant at higher currents when the fuel and oxidant are used at higher rates and the concentration in the gas channel is at a minimum.

2.3 Technical Challenges of PEMFC applications

The PEMFC has the greatest potential as an alternative power source for transportation and stationary applications. However, there are major challenges and limitations that need to address first in order to be feasible for commercialization such as cost, durability, system size, thermal and water management. According to DOE, the following technical hurdles are significantly affects the PEMFC systems. [16]

• Cost

As mentioned above, in order to compete with the internal combustion engine the fabrication costs of fuel cell systems need to be reduced in order to make it commercially viable. To attain this goal, the cost of the platinum (Pt) catalyst needs to be either decreased or substituted with another material, as the major cost component of a PEM fuel cell is the platinum catalyst (Fig. 6). Reducing the amount of platinum required is a major thrust of fuel cell R&D [17].

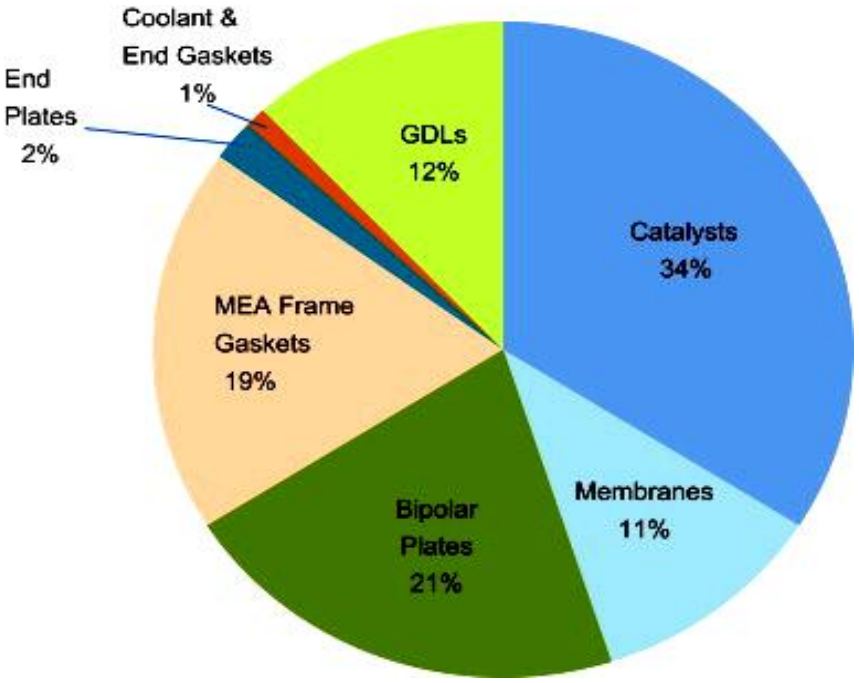

Figure 6. PEM fuel cell stack cost components [18]

Depending on the market price of platinum, the contribution of platinum to the cost of the fuel cell can be 34% or more. As shown in Figure 7, platinum prices can fluctuate entirely on market conditions, which can make it difficult for automobile manufactures to control the costs. If FCEVs enter the market in significant numbers, the demand for platinum will increase, which could lead to increases in platinum prices.

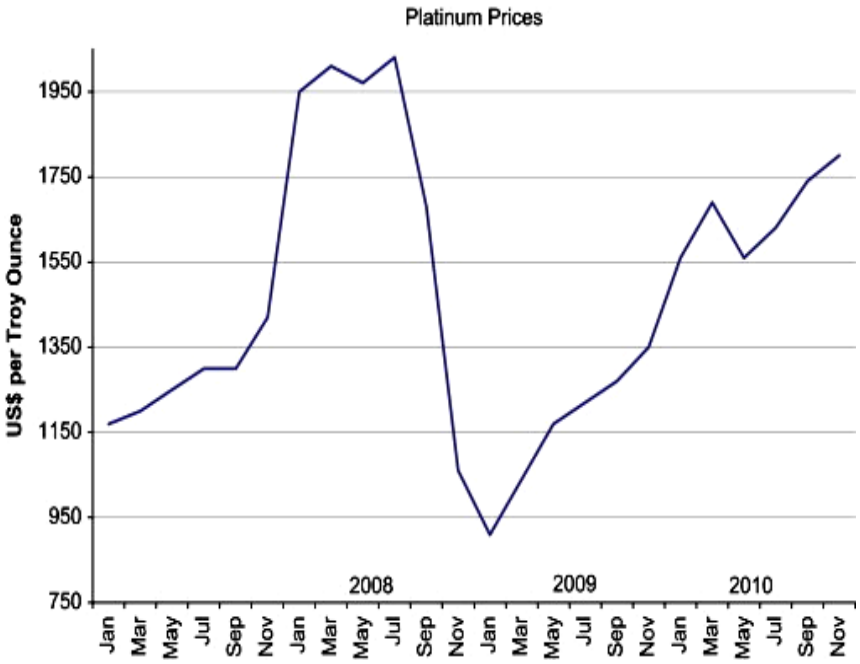

Figure 7. Platinum prices [19]

• Durability and Reliability

Durability is an important issue in proton exchange membrane fuel cells (PEMFCs). Durability appears to be one of the barriers of PEMFC commercialization [20-22]. Oxidant starvation, usually occurring under harsh operating conditions such as sub-zero start-up, rapid load change, and water accumulation during long-term operation is some of the potential factors to result in the degradation of PEMFCs. [23, 24]

In a fuel cell stack, if the oxygen supplied is not enough to maintain the stack current then oxidant starvation will occur. In this case, a reversal of cell voltage could happen. In the absence of oxygen, protons pass through the membrane and combine with each other. Thus, hydrogen is produced to provide the compensatory current [25, 26]. The oxidant starvation behavior of fuel cell has been studied by some researchers [26–29]. Taniguchi *et al*. [29] investigated the

changes of cell voltage, electrode potentials against RHE with time during oxidant starvation and found the inhomogeneous degradation of catalyst. Liu *et al*.

For automotive application, PEMFC systems need to achieve the same level of durability and reliability as current automotive internal combustion engines, which retain 5000 hour lifespan and the ability to operate at freezing conditions (starts from indefinite cold-soak at -20^{o}C and survives from -40 ^{o}C). And for stationary application, PEMFCs are required to reach 40,000 hours of reliable operation in a temperature at -35 ^{o}C to 40 ^{o}C.

• System Size

Compared to internal combustion engine, the size and weight of current fuel cell systems need to be further reduced to meet the packaging requirements for automobiles. This applies not only to the fuel cell stack, but also to the auxiliary components and major subsystems (i.e., fuel processor, compressor/expander, and sensors) making up the balance of power system. [30]

• Improved Heat Recovery Systems

The low operating temperature of PEM fuel cells limits the amount of heat that can be effectively utilized in combined heat and power (CHP) applications. Technologies need to be developed that will allow higher operating temperatures and/or more-effective heat recovery systems, and improved system designs that will enable CHP efficiencies exceeding 80%. Technologies that allow cooling to be provided from the low heat rejected from stationary fuel cell systems (such as through regenerating desiccants in a desiccant cooling cycle) also need to be evaluated. [30]

• Air, Thermal and Water Management

The air compressor or thermal/water management directly influences the performance of PEMFC for automotive applications. Even the small differences between the operating and ambient temperatures necessitate large heat exchange [31]. Furthermore, air management for fuel cell systems is a challenge because today's compressor technologies are not suitable for automotive fuel cell applications. In addition, thermal and water management for fuel cells are issues because the small difference between the operating and ambient temperatures necessitates large heat exchangers.

To achieve these goals, and a viable commercialization of PEMFC systems, requires new innovations and techniques. For example, consider the catalyst which directly supports the anode and cathode chemical reaction and is effectively reflected on the fuel cell performance. It is implicitly assumed that the current density is a function of the morphology and structure of the three-dimensional catalyst layer matrix [32]. Yet, a PEMFCs system uses a noble metal (e.g. platinum) catalyst, for at present, platinum is the only effective catalyst for this system because it is sufficiently reactive in bonding H and O intermediates to facilitate the electrode process. However, as stated earlier, the prohibitive cost of platinum is the greatest commercialization challenge facing PEMFC technology. Additionally, as the GDL allows gas to diffuse from the gas flow channel to the Pt catalyst and allows water to flow away from the catalyst, the GDLs balance water management, electronic conductivity, and mechanical support elements are directly related to PEMFCs functionality. These two components: GDL and

catalyst issues have to be resolved before the developments of PEMFCs are feasible for commercialization.

2.4 Gas Diffusion Layers (GDLs)

PEMFCs require anode and cathode catalyst layers that have excellent electronic contact with current collectors. Moreover, these current collectors must allow ready access of fuel and oxidant to the anode and cathode catalyst surfaces, respectively. These current collectors are called gas diffusion layers (GDLs), which are critical components in achieving high performance in the PEMFC [33]. The requirements of an ideal GDL are the following.

- Effectively transporting the gas reactants to the catalyst layer
- Low electronic resistivity
- Surface that enhances good electronic contact
- Proper hydrophobicity
- Crack free surface morphology and high mechanical integrity to sustain erosion from the gas forces to avoid any particle shading [34]

A recent review of GDLs for PEMFCs by our research group reported different methods to optimize the GDLs performance [35]. In general, the overall porosity of the GDLs, which influences performance—specifically with air as the oxidant—is manipulated by composition as well as the fabrication methods of microporous layers [36]. Synthesis of catalyst supports with high characteristics as well as the good properties of GDLs is required to alleviate the degradation of

PEMFCs. Also reducing the cost along with high power output is an effective strategy to approach PEMFC improvement.

2.5 Surfactant Materials for GDLs

In this research work, two types of anionic surfactants are used, ammonium lauryl sulfate (ALS) in various concentrations, and sodium dodecyl sulfate (SDS). Furthermore, multi-walled carbon nanotubes (MWCNTs) are also used as a support material for GDLs. The term surfactant (“surface-active-agent" or "wetting agent") designates a substance which exhibits some superficial or interfacial activity. The use of surfactant materials has been shown to control particle size and distribution of nanoparticles deposited on carbon support [37, 38, 39]. Furthermore, surfactants on the surface of the particles have an effect on the electrical double layer interactions and on the Van der Waals interactions. Ionic surfactants induce electrostatic interactions, but nonionic surfactants are adsorbed on the surface by steric interactions. Surfactants can increase or decrease the stability of the system.[40] Anionic surfactants are dissociated in water in an amphiphilic (from the Greek word, *amphis*: both and, *philia*: love, friendship) anion, and a cation, which is in general an alkaline metal (Na^+, K^+) or a quaternary ammonium. Anionic surfactants are the most commonly used surfactants.

Sodium dodecyl sulfate (SDS), a water-soluble micelle surfactant, is also used in this study. Sodium dodecyl sulfate has been shown to homogenously disperse carbon nanotubes in water at concentrations above its critical micelle concentration of 8 mM [41, 42]. Sodium dodecyl sulfate has also been used to

control particle size in nanoparticle synthesis [43]. In previous research conducted with Lin *et. al*., SDS was shown as an effective surfactant used to disperse carbon nanotubes in water and also to control platinum particle size during nanoparticles synthesis [38]. Figure 8 shows the self-assembled monolayer structure of SDS micelles on the surface of carbon nanotubes. The hydrophilic (love of water) tail of the SDS micelle attaches to the inert surface of the MWCNT. The negatively charged hydrophobic sulfate head of the micelle repels other micelle capped MWCNTs, overcoming Van der Waals force and allowing dispersion of MWCNTs in water [38].

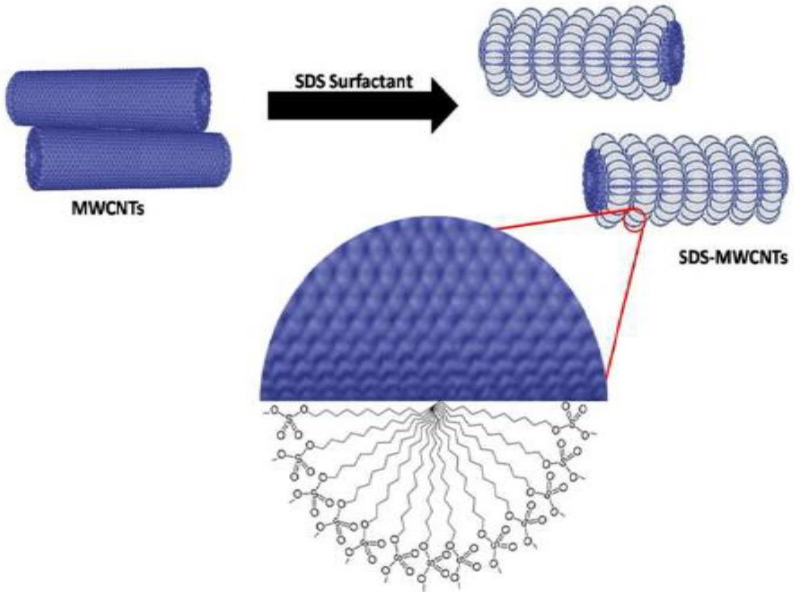

Figure 8 Self-assembled monolayer structures of SDS micelles on MWCNTs [38]

Ammonium lauryl sulfate (ALS), (CH_3-$(CH_2)_{10}$-$CH_2OSO_3NH_4$) is an anionic surfactant. This means it lowers the surface tension of water, making the water spread more easily. As shown in Figure 9, the structural formula at one end of the molecule is a long chain of carbon and hydrogen, while the other end is a salt of sulfuric acid and ammonia. The long chain is hydrophobic, and the salt is hydrophilic, making this a good surfactant.

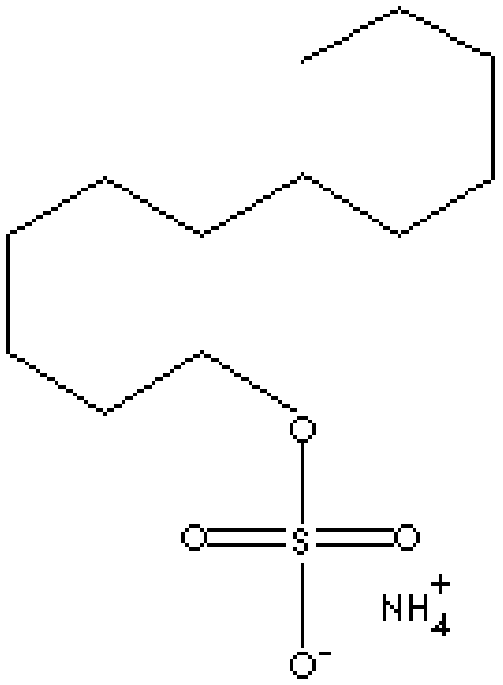

Figure 9. Ammonium lauryl sulfate chemical structure.[44]

In the work study of T. Yalcina *et. al*, the influence of the addition of anionic surfactant ammonium lauryl sulfate (ALS), on the flow properties of bentonite–water systems show an increase of above 10^{-3} mol/l or higher concentrations. This observation is evidence that surfactants adsorbed by clay particles tend to cause aggregation due to interactions between the hydrophilic tails of the

surfactants and the positive edges of the clay particles, which result in the formation of more resistant structures against flowing.

Carbon is an ideal material for supporting nano-sized metallic particles in the electrode for fuel cell applications. No other material except carbon material has the essential properties of electronic conductivity, corrosion resistance, surface properties, and the low cost required for the commercialization of fuel cells. Carbon nanotubes (CNTs) were unexpectedly discovered as a byproduct of fullerenes by direct current (DC) arc discharge; and it becomes today's most promising material in the nanotechnologies. Multi walled carbon nanotubes (MWNTs) were first formed after fullerenes were utilized. Fullerenes, otherwise known as buckyballs (Figure10) [45], is a molecule that consists of 60 carbon atoms (C_{60}) and retains an icosahedral symmetry, which means 60 carbon atoms bonded with each other in 12 pentagons and 20 hexagons. This is the first carbon nanostructure developed by Kroto and his co-workers when they used a pulsed laser beam to evaporate graphite from a rotating disk. [46]

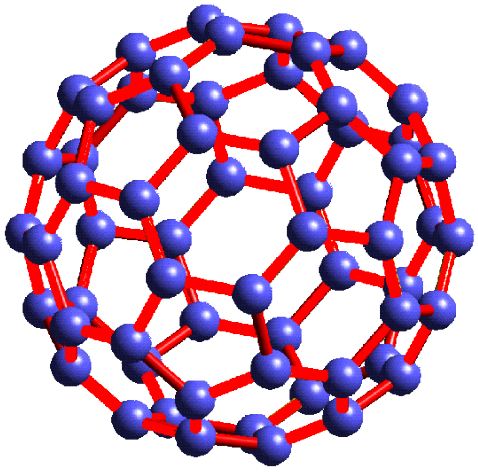

Figure 10 . The icosahedral C60 molecule [44]

MWNTs, as its name implies, are formed multiple graphene sheets (at least two sheets) arranged concentrically into tube structures. Multi walled carbon nanotubes (Figure 11) are formed at relatively lower temperature and at higher temperature than fullerenes-formed single walled carbon nanotubes.

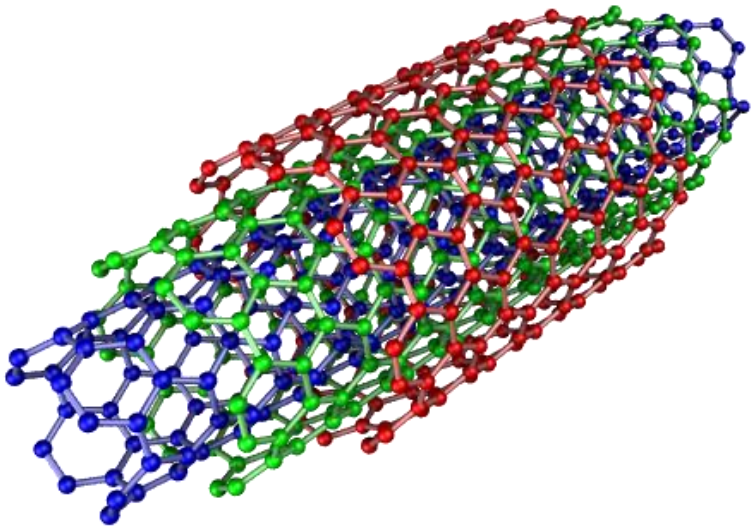

Figure 11. Multiwalled carbon nanotubes [47]

Multi walled carbon nanotubes (MWCNTs) were used as the support materials for GDLs because they possess unique characteristics such as:

- Can be either electrically conductive or semi conductive.
- High electrical conductivity (same as copper).
- High thermal conductivity (some as diamond).
- Superior mechanical strength (100 times greater than steel).

The exceptional qualities of CNTs make it the material of the future. CNTs are extensively applied in various applications such as nanotechnology, electronics, chemical sensors, also sustainability and energy areas including hydrogen storage.

2.6 GDLs Characterizations Techniques

There are two characterization methods of GDLs that influence the fuel cell performance: ex-situ (GDLs alone) and in-situ (within the fuel cells) methods. Various GDL properties, such as electrical and thermal conductivity, porosity, and morphology, can be examined by *ex-situ* methods. The *ex-situ* characterization can be conducted for pristine GDLs or as post-mortem analysis. The results of post-mortem analysis can give secondary information about the possible failure modes in GDLs, if compared against the properties of the pristine sample [48].

The *ex-situ* method may be a very significant as a process control tool; however, *in-situ* methods are critical for understanding the GDLs under actual fuel cell operating conditions. Various GDL properties, such as impedance, water transport, structural deformation and durability, can be examined by *in-situ* methods. These characterization techniques focus on measuring the effect of other components of the PEMFC on the GDL. The *in-situ* characterization of the GDLs can be conducted by assembling and studying the PEMFC single cells. The galvanostatic or potentiostatic polarization methods can be used to characterize GDLs at various RH conditions and temperatures using H2/air in PEMFC single cells. In addition, the following *in-situ* techniques can be used to characterize the GDLs [48]. In this thesis, impedance measurements (*in-situ* methods) were also used to establish a better understanding of factors influencing performance and power loss mechanisms of GDLs. Impedance measurements are also known as Electrochemical Spectroscopy Impedance (EIS). In addition, study the behavior

of GDLs at various RH conditions and temperatures using H_2/ O_2 in PEMFC a single stack cell.

2.6.1 Electrochemical Impedance Spectroscopy (EIS)

Electrochemical Impedance Spectroscopy (EIS), or ac impedance methods, have seen a tremendous increase in popularity in recent years. Initially applied to the determination of the double-layer capacitance [49-52] and in ac polarography [53-55] they are now applied to the characterization of electrode processes and complex interfaces.

In the nineteenth century, Oliver Heaviside created the foundation for impedance spectroscopy through implementation of Laplace transforms application to the transient response of electrical circuits. He also first coined the words *inductance, capacitance,* and *impedance* and introduced these concepts to the treatment of electrical circuits. Heaviside's papers, "The Electrician" were published in 1872 and later printed in book form in 1894. The history of impedance spectroscopy did not start until the year 1894 with the work of Walter H. Nernst. Nernst applied the electrical bridge invented by Wheatstone's measurement of the dielectric constants for aqueous electrolytes and different organic fluids. Nernst's approach was soon employed by others for measurement of dielectric properties and the resistance of galvanic cells.

EIS studies the system response to the application of a periodic small amplitude ac signal. These measurements are carried out at different ac frequencies and, thus, the name impedance spectroscopy was later adopted. Analysis of the system response contains information about the interface, its

structure, and reactions taking place there [56]. However, EIS is a very sensitive technique and it is very often difficult to understand by non-specialists. Frequently, they do not show the complete mathematical developments of equations connecting the impedance with the physico-chemical parameters. EIS is a complementary technique and other methods must also be used to elucidate the interfacial processes.

Electrochemical Impedance Spectroscopy (EIS) is a powerful diagnostic tool that you can use to characterize limitations and improve the performance of fuel cells. There are three fundamental sources of voltage loss in fuel cells: charge transfer activation or "kinetic" losses, ion and electron transport or "ohmic" losses, and concentration or "mass transfer" losses. [76]

Equivalent circuit modeling of EIS data is used to extract physically meaningful properties of the electrochemical system by modeling the impedance data in terms of an electrical circuit composed of ideal resistors (R), capacitors (C), and inductors (L). Because we are dealing with real systems that do not necessarily behave ideally with processes that occur distributed in time and space, we often use specialized circuit elements. These include the generalized constant phase element (CPE) and Warburg element (ZW). The Warburg element is used to represent the diffusion or mass transport impedances of the cell. An example of a generalized equivalent circuit element for a single cell fuel cell is shown below [76].

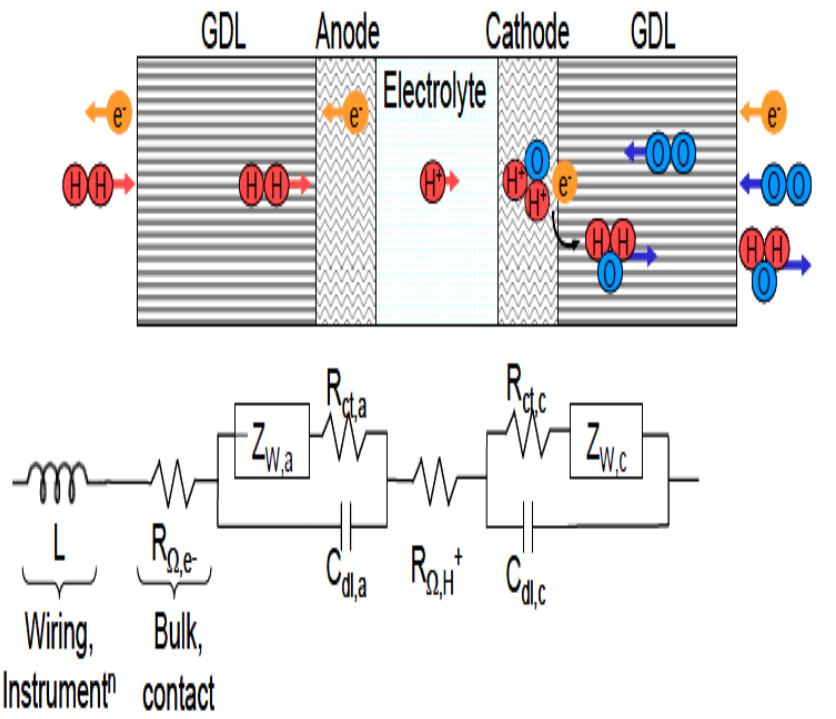

Figure 12. Equivalent circuit element for a single cell fuel cell [76]

In the equivalent circuit analog, resistors represent conductive pathways for ion and electron transfer. As such, they represent the bulk resistance of a material to charge transport such as the resistance of the electrolyte to ion transport or the resistance of a conductor to electron transport. Resistors are also used to represent the resistance to the charge-transfer process at the electrode surface. Capacitors and inductors are associated with space-charge polarization regions, such as the electrochemical double layer, and adsorption/desorption processes at an electrode, respectively [76].

Chapter 3

EXPERIMENTAL

3.1 Gas Diffusion Layer

The gas diffusion layers (GDLs) were fabricated with teflonized non-woven carbon paper as substrate developed by Hollingsworth and Vose (HV) Company, West Groton, MA. The hydrophobic characteristics of the microporous layers were provided by TE5839 Teflon suspension (DuPont, Wilmington, DE) and the Teflon content in the macro-porous carbon paper substrate was about 15 wt. % to avoid flooding by the product water. The vapor grown carbon fiber (VGCF) is nano-fibrous type carbon, which was manufactured by Showa Denko America Inc., New York. The ammonium lauryl sulfate (ALS) (CH_3-$(CH_2)_{10}$-$CH_2OSO_3NH_4$) was acquired from Fisher Scientific, which was used for slurry preparation. The PUREBLACK ® 205-110 Carbon was obtained from Superior Graphite Co., Chicago, IL, USA, that consist of nano-chain that provide improved mechanical strength and adhesion of the microporous layer with macro-porous layer. In order to fabricate the microporous layer, a 0.5 g of carbon powder (75 wt% PUREBLACK carbon powder and 25 wt. % VGCF) was dispersed in 8ml DI water containing various amounts of ALS (150, 320 and 500mM, labeled as sample #s 1, 2 and 3 in Table 1) by sonicating for 30 minutes. The samples then were stirred for 60 minutes using magnetic stirrer. PTFE (25 wt. %) dispersion was added into the mixture and followed with the magnetic stirring for about 10 minutes. The carbon slurry was coated onto the nonwoven carbon paper substrates

using Easycoater equipment (EC26, Coatema) with the velocity of 3.0 $m.min^{-1}$ as depicted by Kannan et al. [57]

The carbon loading on the micro-porous layer was about $3mg/cm^2$, controlled by the wire thickness on the wire rod. After coating the micro-porous layer, the GDL samples were dried at room temperature overnight and then sintered at 350°C for 30 minutes. A GDL sample was washed to remove the ALS impurities by immersing them in warm de-ionized (DI) water for 30 minutes.

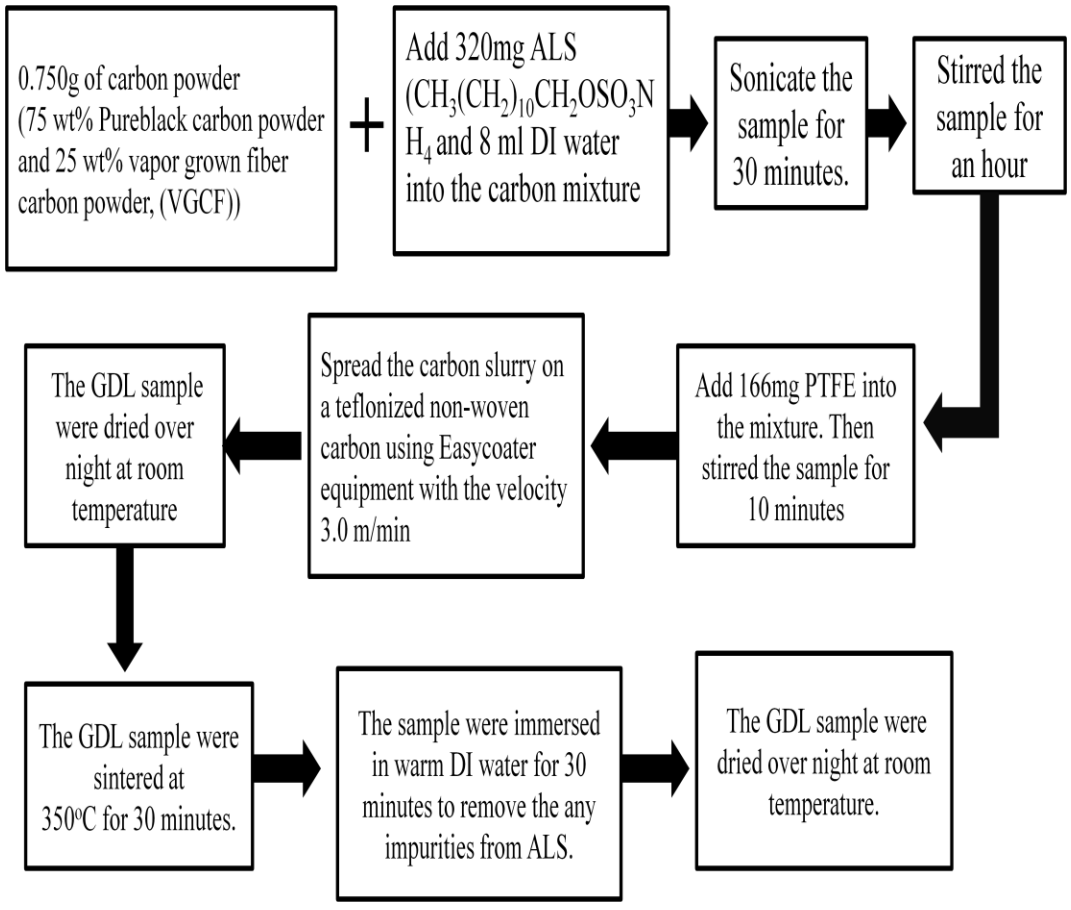

Figure 13. Fabrication process of ALS based GDL

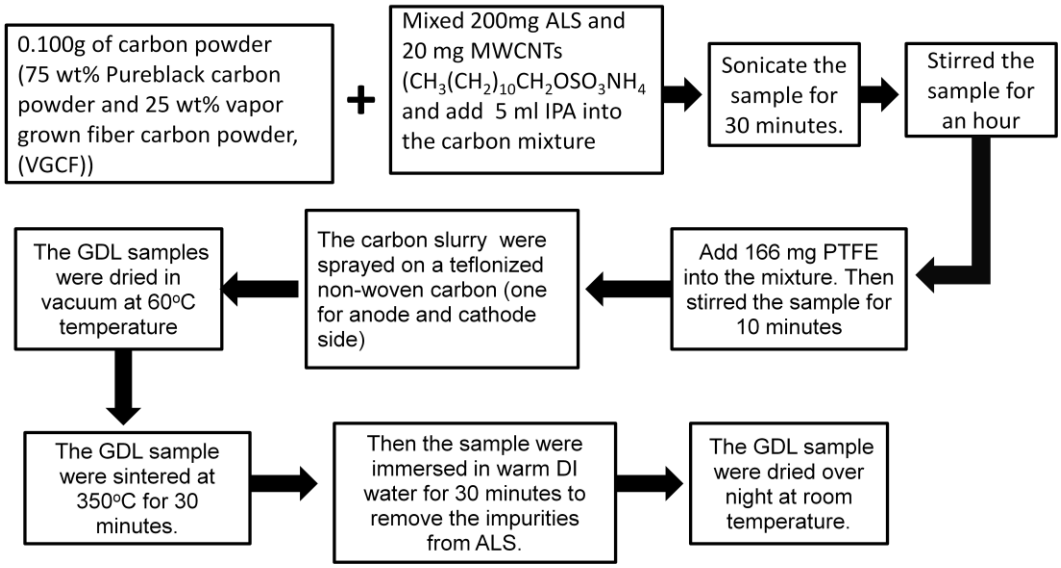

Figure 14. Fabrication process of MWNTs with ALS based GDL

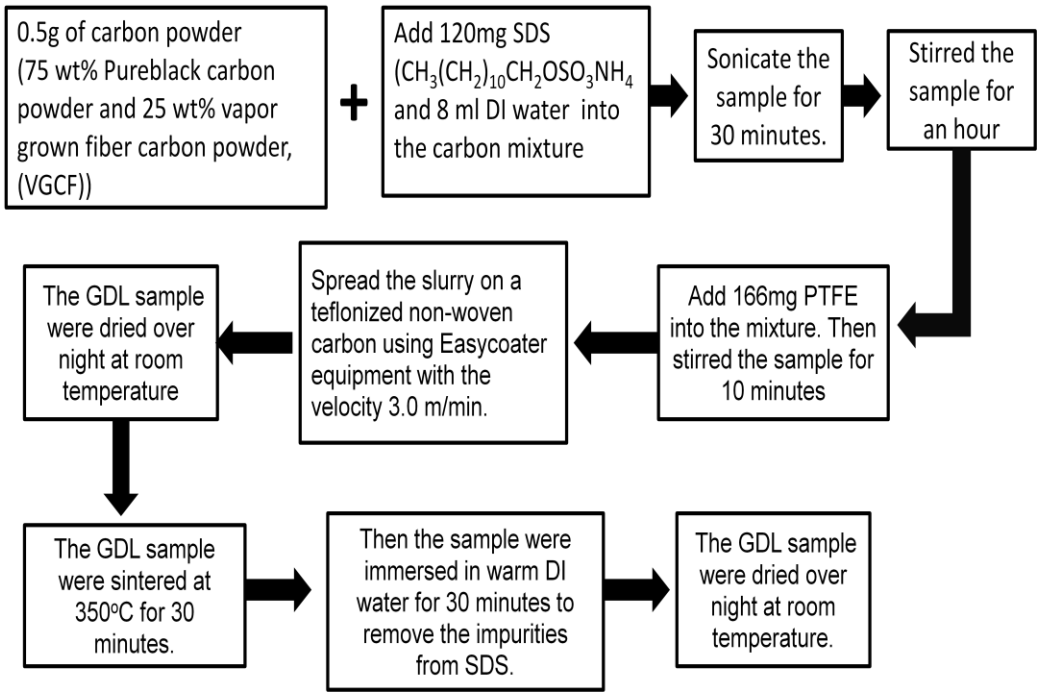

Figure 15. Fabrication process of SDS based GDL

TABLE II.

GDL sample was fabricated with different concentration of ALS.

SAMPLE	PUREBLACK (mg)	VGCF (mg)	DI WATER (ml)	PTFE (mg)	ALS Amount (mg)
1	375	125	8	166	150
2	375	125	6	166	300
3	375	125	8	166	500
4	562.5	187.5	8	166	320

TABLE III.

Composition of SDS and ALS for comparison and evaluation

SAMPLE	NAME	PUREBLACK (mg)	VGCF (mg)	DI WATER (ml)	PTFE (mg)	ALS Amount (mg)
1	SDS	375	125	8	166	120
2	ALS	562.5	187.5	6	150	320

Figure16. Easycoater equipment (EC26, Coatema)

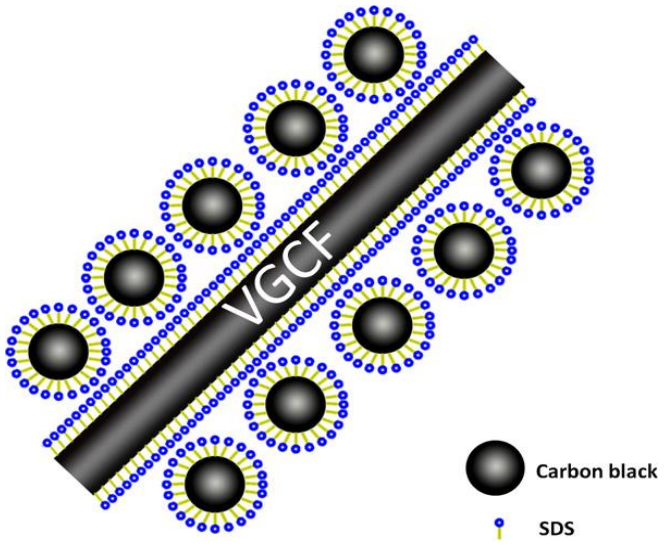

Figure 17. Schematic representation of micelle-encapsulated Pureblack and VGCF carbons [58]

3.2 Catalyst Coated Membrane

Catalyst-coated membranes (CCM) with 5 cm^2 active area were fabricated using Pt/C catalyst slurry in isopropanol (20 ml for 1 g of electrocatalyst) by the micro-spray method for anode and cathode sides on Nafion® membrane (NRE 212, Ion Power Inc., New Castle, DE, USA). The isopropanol was added after purging the catalyst powder in flowing nitrogen gas for about 30 minutes to avoid any flame/ignition. In order to extend the reaction zone of the catalyst layer, 5% Nafion® solution from Ion Power Inc., New Castle, DE, USA (30 wt% to Pt catalyst; 10 ml Nafion solution for 1 g of electrocatalyst) was added to the catalyst slurry. The membrane was fixed in a home-made fixture to ensure the anode and cathode catalyst layers are on exactly the same area of the membrane. The catalyst loadings on the anode and cathode sides were about 0.4 mg Pt/C per cm^2, respectively. Figures below (Figures 17a and 17b) show the process of spraying the CCM. The catalyst coated Nafion-212 membrane was vacuum dried at about 60^oC for 15 minutes before assembling it in the single stack fuel cell test system.

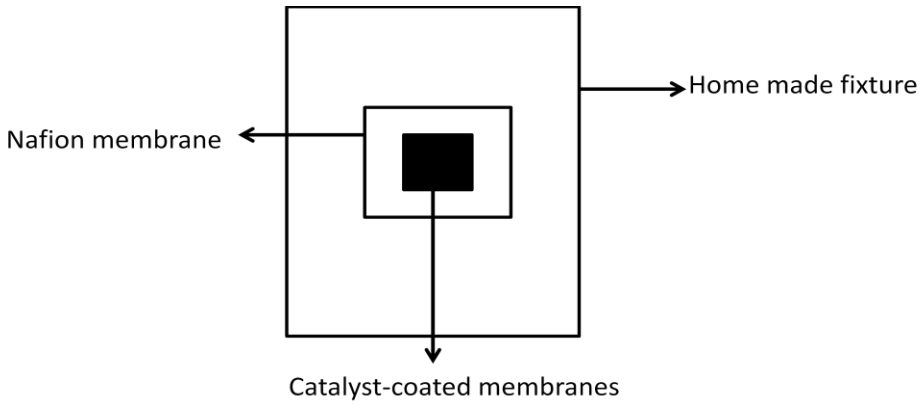

Figure 18a. Homemade fixture for CCM

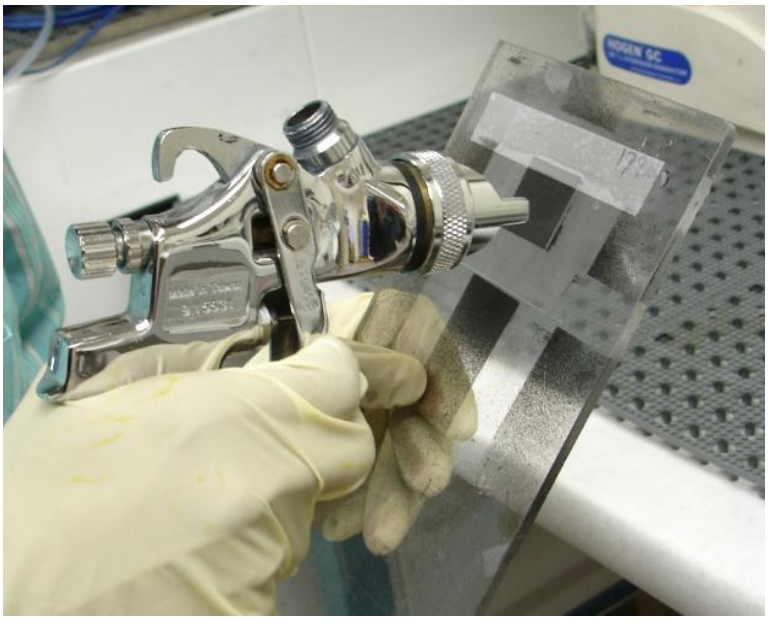

Figure 18b. CCM micro-spray method

3.3 Membrane Electrode Assembly and Fuel Cell Performance

Fabrication of the membrane electrode assembly (MEA) consisting of a commercial catalyst (Pt/C) coated on both the anode and cathode sides of the Nafion-212 membrane (Ion Power Inc., New Castle, DE, USA) was reported elsewhere [57]. Briefly, catalyst ink was prepared by adding IPA (20 ml for 1 g of electrocatalyst) after purging the Pt/C catalyst powder (TKK, Japan) in flowing nitrogen gas for about 30 minutes to avoid any flame or ignition. In order to extend the reaction zone of the catalyst layer, 5 wt. % Nafion® (Ion Power Inc., New Castle, DE, USA) dispersion (10 ml for 1 g of electrocatalyst) was added to the catalyst slurry. A catalyst layer on the Nafion membrane with 5 cm^2 active area was fabricated on both sides by spraying the catalyst ink using the micro-spray method. For both anode and cathode, the catalyst loadings were about 0.4mg Pt/C cm^{-2}, respectively. The MEA was vacuum dried at 60^oC for 15

minutes before assembling the electrode in the single cell test cell. The MEA was assembled by sandwiching inside a single test cell (Fuel Cell Technologies Inc, Albuquerque, NM, USA) along with the GDLs on both sides. Gas sealing was achieved using silicone coated fabric gaskets (Product # CF1007, Saint-Gobain Performance Plastics, USA) and with a uniform torque of 0.45Nm to seal the single stack test cell. The single stack fuel cell performance was evaluated at 80^{o}C with various relative humidity (RH) conditions and ambient pressure with H_2/O_2 and H_2/air by using Greenlight Test Station (G50 Fuel Cell System, Hydrogenics, Vancouver, Canada) with fixed flow rates of 200 SCCM on the anode side (H_2) and 300 SCCM on the cathode side (O_2 or air). The flow tracking modes were not used. The RH of the reactant gases were maintained at different values (60, 70, 80, 90 and 100 %RH) by controlling the humidity temperature.

The Greenlight Test Station (G50 Fuel Cell System, Hydrogenics, and Vancouver, Canada) is shown in Figure 18.

Figure 19. Greenlight Test Station (G50 Fuel Cell System, Hydrogenics, Vancouver, Canada)

3.4 Optimizing GDLs Properties

The optimization of GDLs and its properties were identified in other research. The main focus of this work is mainly on the effects of different materials for carbon slurry and dispersion for optimum GDL performances. In the previous studies [59, 60] and other literatures [61, 62], the parameters of PTFE and carbon loadings were investigated and the optimized values of PTFE percentage weight (wt. %) and carbon slurry were directly given as illustrated in Figure 19.

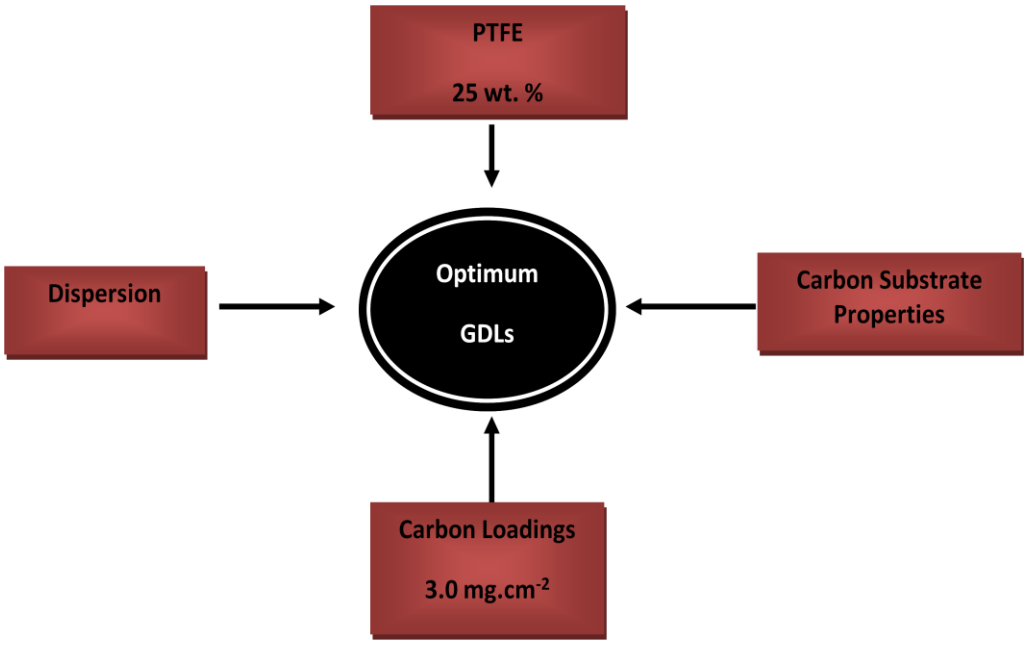

Figure 20. Diagram of improving parameters of GDLs [62]

Chapter 4

RESULTS AND DISCUSSION

4.1 Fuel cell performance of GDL Samples with ALS, MWCNTs and SDS Base

It was investigated in numerous studies [64-67] that the proper compositions of carbon black containing 75 % wt. Pureblack and 25 % wt. of nano-fibrous carbon with 25 wt. % of PTFE were uniformly distributed. This composition provided the maximum performance with air and oxygen as an oxidant at various relative humidity levels for PEMFCs. Moreover, the carbon loadings on micro-porous layer were maintained at 2.5 to 3.0 $mg.cm^{-2}$. These parameters were also found to be successful in this study.

Various concentrations of ALS based GDL were evaluated for PEMFC performance with the following sets of conditions: H_2/O_2, H_2/Air, constant temperature of 80^oC and different relative humidity (RH) conditions (60, 70, 80, 90 and 100% RH). Moreover, the flow rate was set to 200 and 300 SCCM for the anode and cathode. The catalyst coated membrane loading using a commercial catalyst (Pt/C) was kept at $0.4mg.cm^{-2}$ for both the anode and cathode. As presented in Table II, the four samples (#1, 2, 3, and 4) were prepared at different concentrations of ammonium lauryl sulfate (ALS); 150, 300, 500 and 320mg. Figure 21 shows that sample #4 obtained the highest peak power output of 1300 $mW.cm^{-2}$. It was determined and achieved that 75:25 (at 0.750g) ratio of Pureblack and VGCF, and 320mg of (30 wt. % solution) of ALS is the optimal concentrations to achieve the maximum power output.

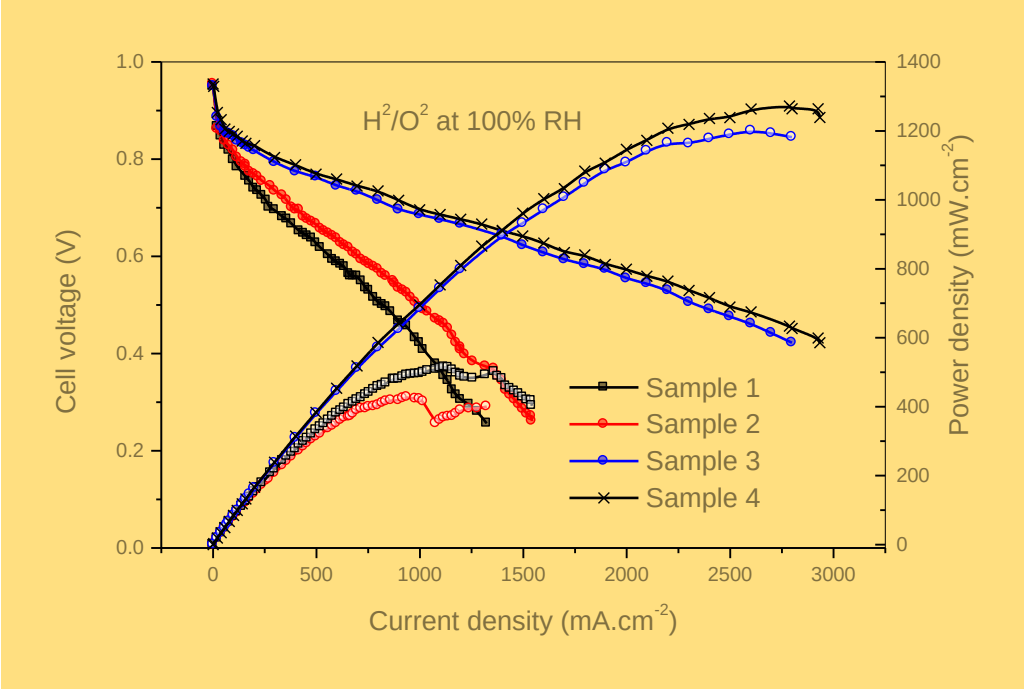

Figure 21. Fuel cell performance of various ALS concentration at 80°C.

Based on the PEM fuel cell performance of various GDL samples, ALS, MWCNTs, and SDS, were compared using these sets of conditions: H_2/O_2, H_2/Air, constant temperature of 80°C and different relative humidity (RH) conditions (60, 70, 80, 90 and 100% RH). MWCNTs have a different concentration, which is 75 wt. % Pureblack and 25 wt. % nano-fibrous VGCF at 100 milligram. The output for these conditions is depicted in individually in Figures 22-28. In comparing all the samples (Figure 27), the GDL with the ALS based sample in the above set of conditions demonstrated and obtained the highest power density value of 1000 mW/cm^2 for 60 % RH and 1300 mW/cm^2 for 100% RH for H_2/O_2 . The same ALS sample was evaluated for H_2/Air and shows a high power density of at various RH conditions (60, 70, 80, 90 and 100% RH),

as Figure 23 illustrates. The figure also shows that at 100% and 60 %RH, the power output density is about 500 mW/cm^2 and 350 mW/cm^2, respectively.

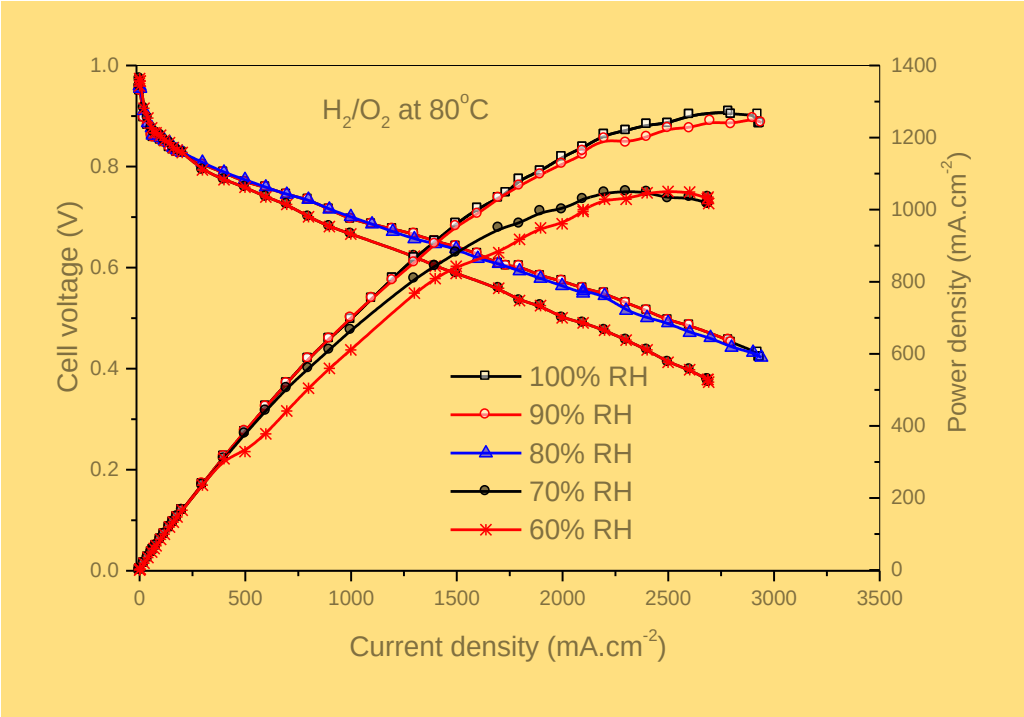

Figure 22. ALS fuel cell performance at different RH conditions using H_2/O_2.

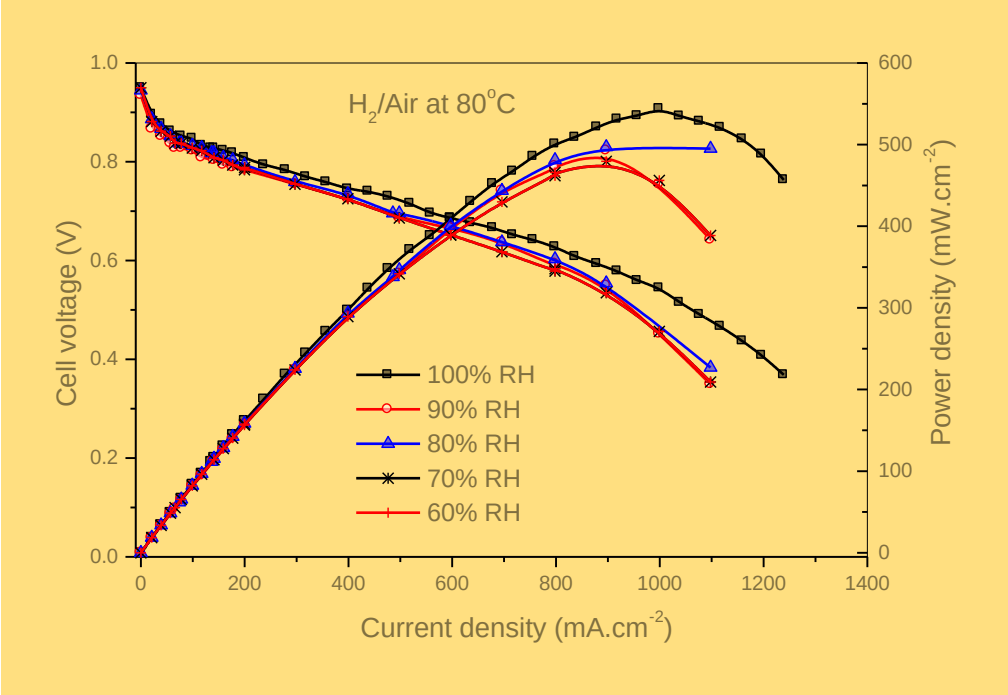

Figure 23 . ALS fuel cell performance at different RH conditions using H_2/Air

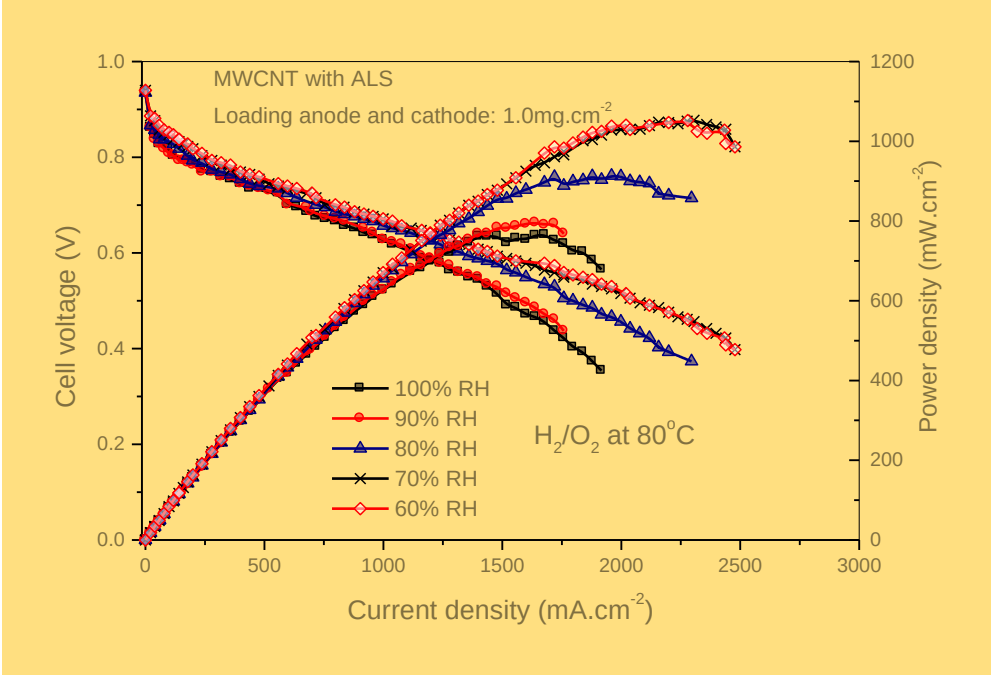

Figure 24. MWCNTs with ALS fuel cell performance at different RH conditions using H_2/O_2

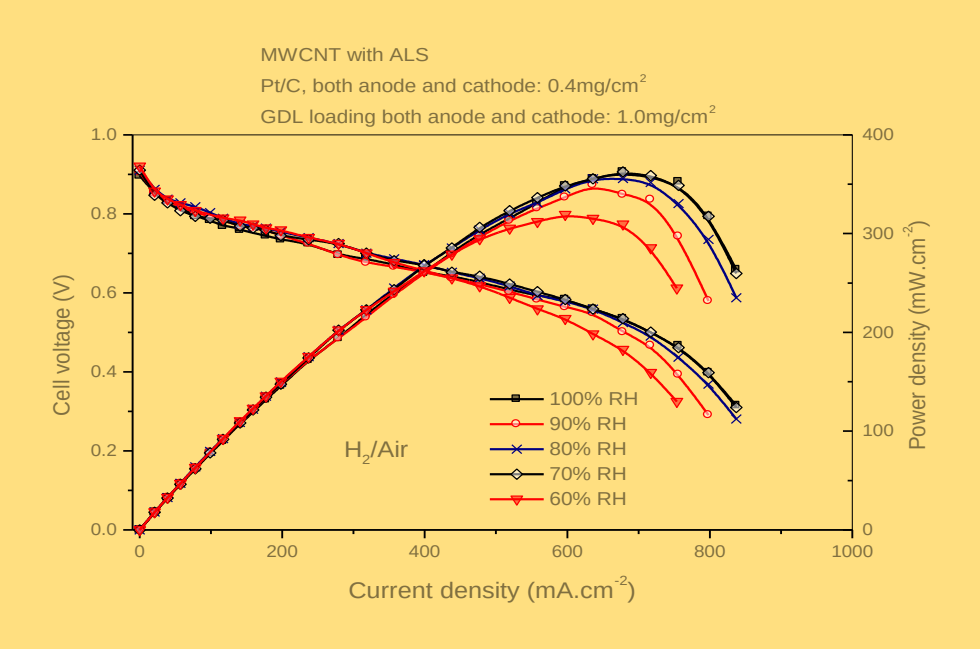

Figure 25. MWCNTs with ALS based at different RH conditions using H_2/Air conditions.

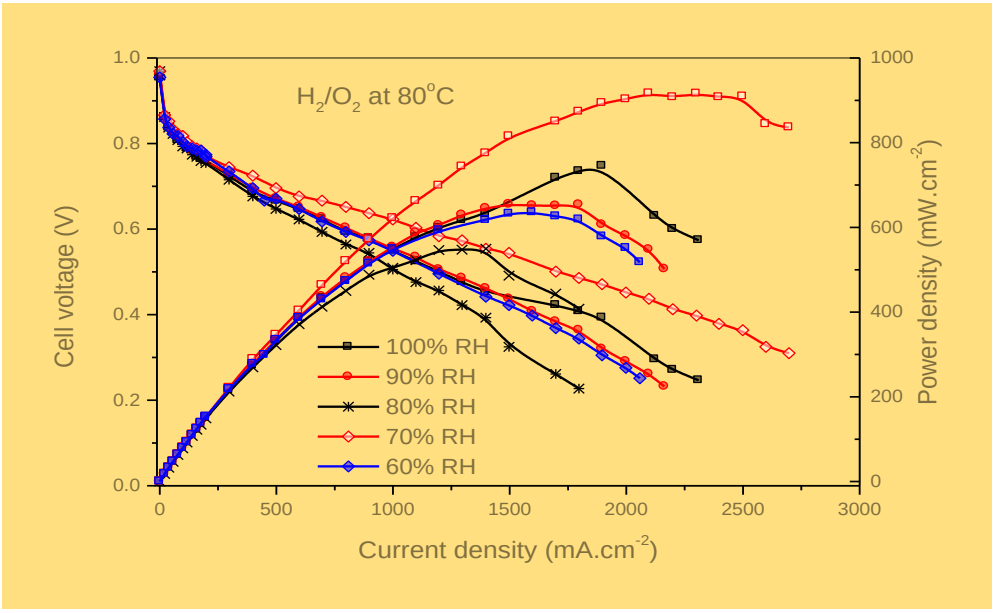

Figure 26. SDS fuel cell performance at different RH conditions using H_2/O_2

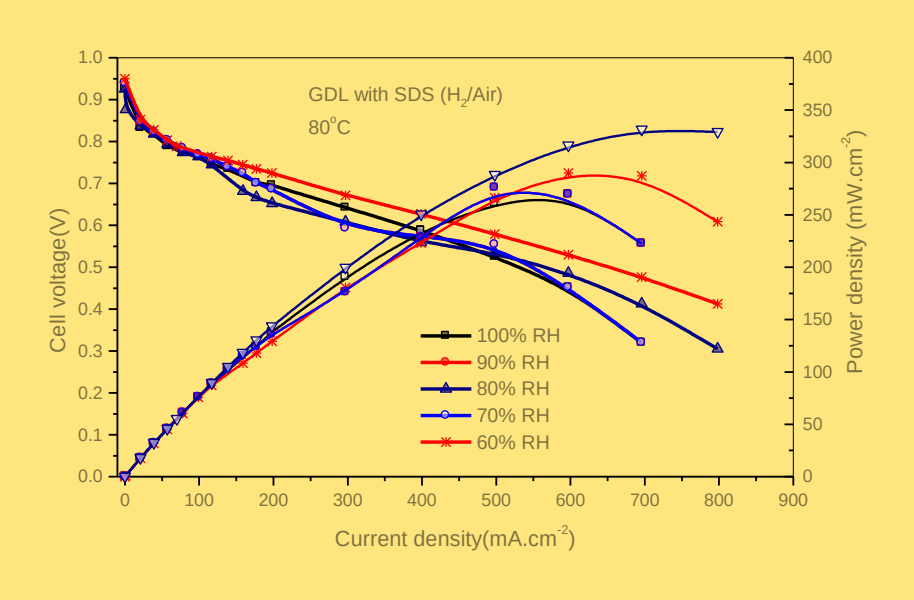

Figure 27. SDS fuel cell performance of at different RH conditions using H_2/Air

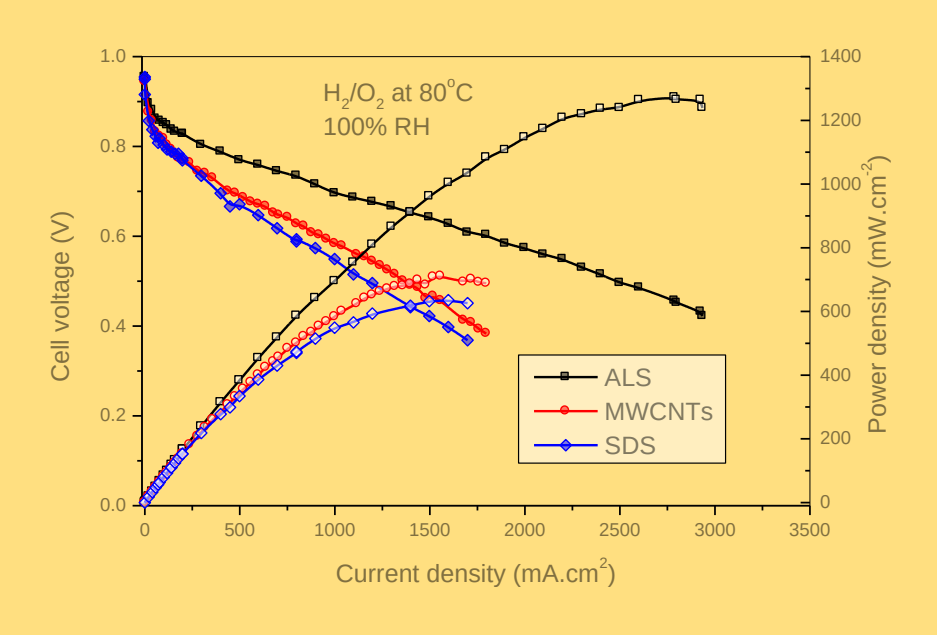

Figure 28. Fuel cell performance of ALS, MWCNTs and SDS.

TABLE IV

Fuel Cell Performance Summary of ALS, MWCNTs and SDS at 80^{o}C, H_2/O_2 and H_2/Air.

Sample	% Composition		Power density ($mW.cm^{-2}$)	Power density ($mW.cm^{-2}$)
	Pureblack	VGCF	H_2/O_2	H_2/Air
ALS	75	25	1300	500
MWCNTs	75	25	1100	260
SDS	75	25	850	230

Table IV compares all the GDL samples, ALS, MWCNTs and SDS. The fuel cell performance was evaluated at 80^{o}C using air and oxygen as oxidants. Furthermore, all the samples tested had the same anode and cathode thickness. It is evident that the ALS sample shows the highest peak power density for both H_2/O_2 and H_2/Air. SDS and MWCNTs demonstrates the lowest power density using air and oxygen as oxidants at 100% RH. However, MWCNTs and SDS exhibit (see figure 23 and 25) the highest performance at 60 and 70% RH, with a peak power density of 1100 and 850 $mW.cm^{-2}$. This means that the gas diffusion characteristics of these two samples were optimum at 60 and 70 % RH with high limiting current density range.

4.2 EIS Analysis of ALS, MWCNTs and SDS

The GDL is the critical component for the mass-transport process within the electrode. By using impedance spectroscopy, Springer *et al*. [68] proved that at low overpotential, at which the ORR kinetics predominates the electrode

process, the cathode performance was somewhat improved with the use of a double gas diffusion layer. At high overpotential, at which mass transfer is the limiting factor, the substantially large mass transfer loop develops for the case of a double gas diffusion layer.

Many studies [69–72] have demonstrated the importance of the morphology of the gas diffusion layer. Kong et al. [73] made a great effort to understand the influence of pore-size distribution of gas diffusion layers on mass transport using the AC impedance technique. Fisher *et al*. [74] report using a pore forming step, conducted with a pore-former, for the purpose of examining the influence of pore-size distribution of the gas diffusion layer on the cell performance. The cell performance improved after the introduction of this process to the catalyst layer. The effect of the pore-forming process on mass-transport limitation was attributed to the increased porosity of the catalyst layer. The low-frequency feature of the Nyquist plots indicated that the content of the pore-former did have a large influence on the mass transfer, and there existed an optimum amount *(*7mg/cm^2*)* of pore-former or an appropriate macro pore volume of the gas diffusion layer.

EIS helps in measuring the transport properties in fuel cells, especially the ionic conductivity of the membrane; it helps in measuring the overall impedances at the cathode side and anode side, and the fuel cell as a whole. In order to carry out this analysis, we make use of equivalent circuit models wherein physiochemical processes occurring within the fuel cell are represented by a network of resistors, capacitors and inductors through which we can extract

meaningful qualitative and quantitative information regarding the sources of impedance within the fuel cell.

There are three fundamental sources of voltage losses in fuel cells: charge transfer activation or “kinetic” losses, ion and electron transport or “ohmic” losses, and concentration or “mass transfer” losses. These losses are associated with different chemical processes taking place inside the cell which have different characteristic and time constants, and hence they are exhibited at different AC frequencies. When conducted over a broad range of frequencies, impedance spectroscopy can be used to identify and quantify the impedance associated with these various processes.

In general, in fuel cells, the high-frequency region (>100 Hz) of an impedance spectrum reflects the charge transport in the catalyst layer, whereas the low-frequency region (0.01 Hz, in general) represents mass transport in the GDL, the catalyst layer, and the membrane. In this thesis, we are trying to understand and analyze the effects of using different materials in the gas diffusion layer, especially understanding the resistance effects at different layers by carrying out EIS experiment.

Humidity plays a very important role in determining the performance of polymer electrolyte membrane (PEM) fuel cells. Low humidity impacts the fuel cell by increasing the high frequency resistance of the cell, which is dominated by the membrane resistance, and indicates that the conductivity membrane decreased at lower humidity. To ensure that we take out this variability, all the

measurements were carried out at 100% relative humidity. Hence the measurements become independent of the humidity factor.

In this research study, the EIS method was performed to find the internal impedances of GDL samples with different RH conditions at 80°C using H_2/O_2 and H_2/Air. In addition, all the samples were evaluated at open circuit voltage. Figure 29-31 illustrates the Nyquist plot for MWCNTs, SDS and ALS samples. In the Nyquist impedance plot, the imaginary part of impedance is plotted as a function of its real component in the frequency range from <10 kHz to 1 mHz.

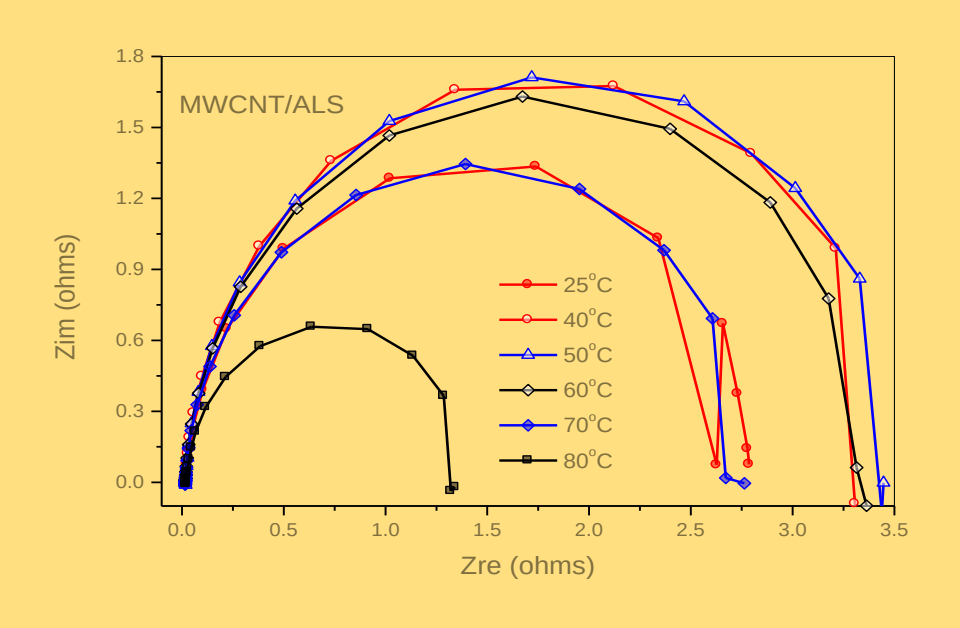

Figure 29. Electrochemical Impedance Spectroscopy of MWCNTs with ALS.

As depicted on figure 29, in ALS based MWCNTs, the single semi-circle loop indicates the interfacial kinetics of the cell while the diameter shows the charge transfer resistance of the cell. The charge transfer resistance varies at different temperatures. Figure 29 shows that at 80°C the cell exhibits the lowest

charges transfer resistance compared to the temperatures starting from 25 to 70^{o}C. Furthermore, the impedance spectra shows the semi-circle loops- at higher frequency of 6kHz determined by charge transport in the catalyst layer and the lower frequency (0.5mHz) loop determined by charge transport in the gas diffusion layer. The impedance behavior of a PEMFC cathode catalyst layer is considered and governed by two transport process, proton migration and oxygen diffusion.

As we can observe from the above data, for high temperature operation of the fuel cell tested at 80 ^{0}C, there is a resistance at higher frequencies which is associated with charge transport layer at the catalyst layer. But at lower frequencies, we observe zero impedance with respect to the impedance level due to mass transport at the GDL, catalyst layer and the membrane. The efficiency and durability of the polymer membrane inside the fuel cell are maximized at about 80^{0}C. PEMFCs show optimum performance at an operating temperature of about 80^{o}C. However, as the operating temperature is lowered, we observe a resistance spread across the wide frequency range indicating lower performance of the fuel cell. Interestingly, CNT-GDL had better electrical conductivity and mass transfer ability than those of Toray GDL. The higher hydrophobic property of GDL with CNT on carbon fiber with covalently assembled metal nanocatalysts was diagnosed by EIS. [75]

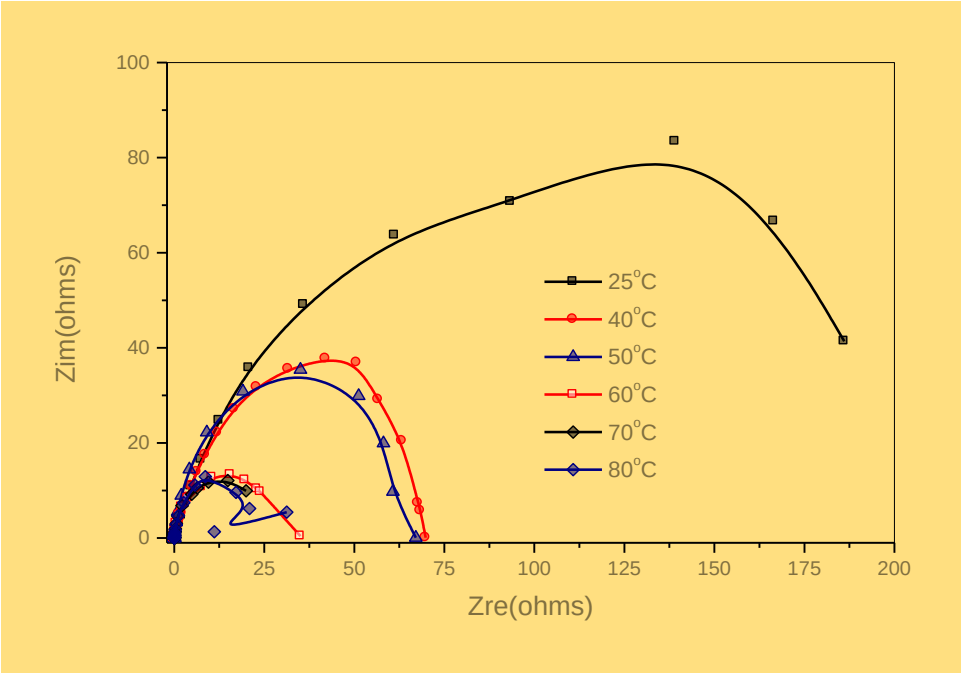

Figure 30. Electrochemical Impedance Spectroscopy of ALS.

Figure 30, shows the EIS measurements for ALS. The impedance measurements at different operating temperatures show a similar trend as the above graph, but the resistance values for the ALS gas diffusion layer are very high compared to the gas diffusion layer containing ALS based MWCNT, demonstrating the absence of conductivity/ more resistivity. This results in degrading performance of the fuel cell in terms of its efficiency and current density. The frequency range used for the analysis was from 6 kHz to 1 mHz.

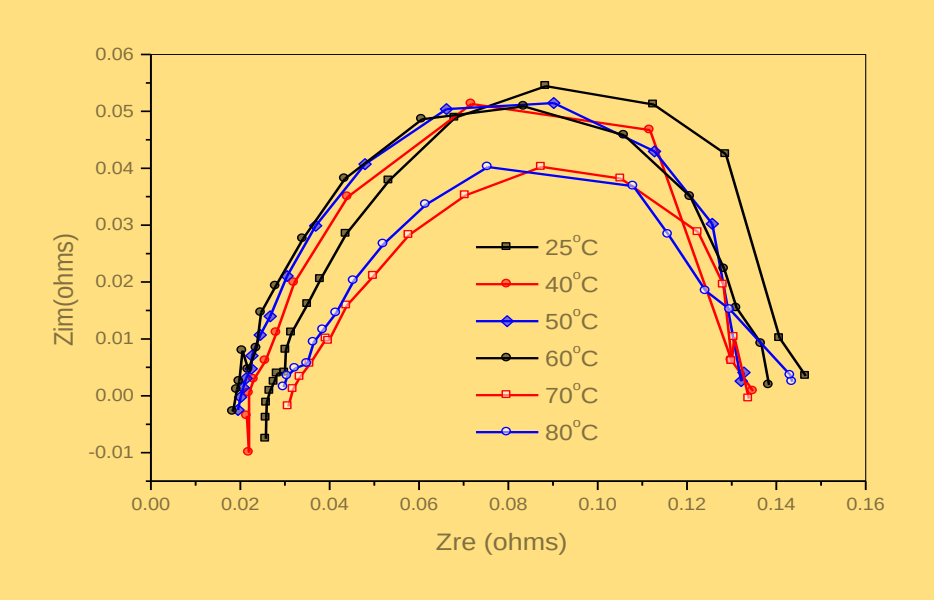

Figure 31. Electrochemical Impedance Spectroscopy of SDS.

Figure 31 demonstrates the collected EIS measurements for SDS. As we can discern, the impedance tends to vary comparably similar irrespective of the operating temperature. This means that SDS material is independent of temperature variations or the operating temperature of the fuel cell. The temperature variation from 25^{o}C to 80^{o}C has little or no effect on the impedance of the half-cell/electrode cell. In this figure, the frequency range was set from 10 kHz to 5 mHz.

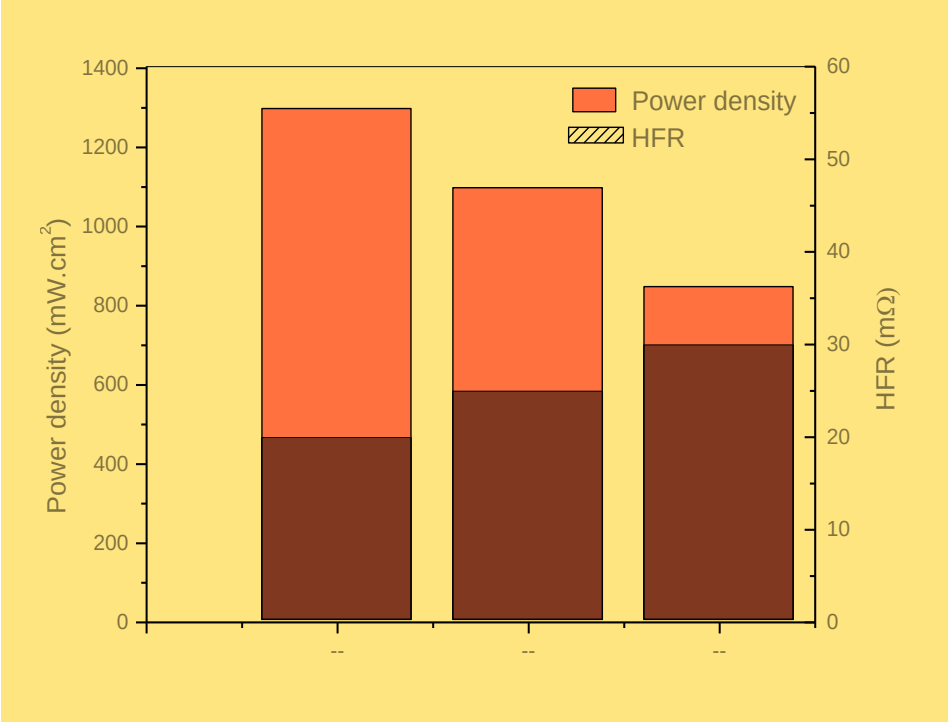

Figure 32. Fuel cell performance and electrochemical impedance spectroscopy (EIS) of ALS, ALS+MWCNTs and SDS

As indicated in figure 32, the fuel cell performance and electrochemical impedance spectroscopy of ALS, MWCNTs with ALS and SDS. The highest peak power density obtained were 1300mW.cm^2 , 1100mW.cm^2 and 850mW.cm^2 for ALS, MWCNTs with ALS and SDS. For the high frequency resistance (HFR), the measurements achieved for the three materials used were 20mΩ (ALS), 25mΩ (MWCNTs with ALS) and 30mΩ (SDS). The results indicate that humidity plays a critical role in determining the performance of polymer electrolyte membrane (PEM) fuel cells. This means that the conductivity of bulk electrolyte membrane will decreased at lower humidity when the HFR of the cell increased.

Chapter 5

CONCLUSION

GDLs are a critical and essential part of the PEMFCs. They carry out various important functions such as transportation of reactants to and from the reaction sites. The material properties and structural characteristics of the substrate and the MPL strongly influence the fuel cell performance. The GDLs' performance was evaluated through *in-situ* methods, polarization curve and electrochemical impedance spectroscopy under PEMFC conditions. These conditions were evaluated using different GDL samples (ALS, MWCNTs and SDS) at different relative humidity (RH) using air and oxygen as a oxidant. In addition, various temperatures were evaluated in impedance measurements of ALS, MWCNTs and SDS.

GDLs were fabricated with different materials to compose the microporous layer to evaluate the effects on PEMFC power output performance. The consistency of the carbon slurry was achieved by adding 25 wt. % of PTFE, a binding agent with a 75:25 ratio of carbon (PUREBLACK and VGCF). The GDLs were investigated in PEMFC under various RH conditions using H_2/O_2 and H_2/Air. All the samples conducted have the same thickness for both anode and cathode side. It is evident that the ALS sample showed the highest peak power density of 1300 and 500mW.cm^{-2} for both H_2/O_2 and H_2/Air. SDS and MWCNTs demonstrates the lowest power density using air and oxygen as oxidants at 100% RH, as shown in Table IV. However, MWCNTs and SDS exhibits (see Figures 24 and 26) the highest performance at 60 and 70% RH with a peak power density of

> 800 $mW.cm^{-2}$. This means that the gas diffusion characteristics of these two samples were optimum at 60 and 70 % RH with high limiting current density range.

EIS aids in measuring the transport properties in fuel cells, especially the ionic conductivity of the membrane; it helps in measuring the overall impedances at the cathode side, anode side and the fuel cell as a whole. There are three fundamental sources of voltage losses in fuel cells: charge transfer activation or "kinetic" losses, ion and electron transport or "ohmic" losses, and concentration or "mass transfer" losses. These losses are associated with different chemical processes taking place inside the cell which have different characteristic time constants and hence they are exhibited at different ac frequencies. The EIS method was performed to find the internal impedances of GDL samples with different RH conditions at 80^oC using H_2/O_2. In addition, all the samples were evaluated at open circuit voltage. The three samples demonstrated different performance at various temperatures. As shown in figure 29-31, we can observe from the above data, for high temperature operation of the fuel cell that is at 80^0C, there is a resistance at higher frequencies which is associated with charge transport layer at the catalyst layer. However at lower frequencies, we observe no impedance which is the impedance level due to mass transport at the GDL, catalyst layer and the membrane. The efficiency and durability of the polymer membrane inside the fuel cell are maximized at about 80 ^0C. PEMFCs show optimum performance at an operating temperature of about 80ºC. However, as the

operating temperature is lowered, we observe a resistance spread across the wide frequency range, indicating lower performance of the fuel cell.

This thesis work utilized different materials (ALS, MWCNTs and SDS) to compose the microporous layer of GDLs, and evaluated the effects on PEMFC power output performance through a polarization curve/graph and electrochemical spectroscopy impedance measurements. GDLs are important part of the MEA for the PEMFCs and there are other materials that provide interesting and promising results for future:

- The study of graphene structure, which shows a potential for high power density for PEMFC.
- Evaluate the fuel cell performance of graphene with different loadings on the GDLs.
- Further investigations of ALS with different percent composition of carbon and evaluate ALS based MWCNTs using different loadings on GDLs. Moreover, investigate various weigh percent of PTFE on MWCNTs with ALS base.
- In addition, the thesis work done can be evaluated under various RH conditions using H_2/O_2 and H_2/Air for EIS.

REFERENCES

[1] Spiegel, Colleen S. "Designing & Building Fuel Cells". McGraw Hill: New York. 2007. pg. 4

[2] Larminie, James and Andrew Dicks . "Fuel Cell Systems Explained". Chichester, England; Hoken, NJ: J. Wiley, 2003. pg.15.

[3] Comparison of Fuel Cell Technologies. U.S. Department of Energy Hydrogen Program. http://www1.eere.energy.gov/hydrogenandfuelcells/fuelcells/pdfs/fc_comparison_chart.pdf

[4] "Fuel cell". *Encyclopædia Britannica. Encyclopædia Britannica Online.* Encyclopædia Britannica Inc., 2012. Web. 23 May. 2012 http://www.britannica.com/EBchecked/topic/221374/fuel-cell.

[5] U.S Department of Energy Hydrogen Program, 2009 Mar. Available: http://www1.eere.energy.gov/hydrogenandfuelcells/pdfs/doe_h2_program.pdf

[6] L. Cindrella, A.M. Kannan, J.F. Lin, K. Saminathan, Y. Ho, C.W. Lin and J. Wertz. "Gas diffusion layer for proton exchange membrane fuel cells-A review". Journal of Power Source 194(2009) 146-160. http://www.sciencedirect.com.ezproxy1.lib.asu.edu/science/article/pii/S0378775309006399

[7] *Federal &State Incentives & Laws*. 2011. http://www.afdc.energy.gov/afdc/laws/laws/AZ/tech/3255]

[8]. L.R Jordan, A.K. Shukla, T. Behrsing, N.R. Avery, B.C. Muddle, M. Forsyth, J.Appl. Electrochem. 30(2000) 641-646.

[9] M. Neegrat, , A.K. Shukla, J. Power Sources 104(2002) 289-294.

[10] *Hydrogen Fuel Cells are Not New*. 2012. http://www.mycoolelectriccar.com/hydrogen-fuel-cells.html

[11] Q. Yan, H. Toghiani, H. Causey, J. Power Sources 161 (2006) 492–502

[12] Los Alamos National Laboratory, "Fuel Cells-Green Power". http://www.lanl.gov/orgs/mpa/mpa11/Green%20Power.pdf

[13] Jain,Rishabh and Biswajit Mandal. *Studies on Ideal and Actual Efficiency of Solar Polymer Electrolyte Fuel Cell*. 2012. http://www.altenergymag.com/emagazine.php

[14] J. Xie, D.L. Wood III, D.M. Wayne, T.A. Zawodzinski, P. Atanassov, R.L. Borup, J. Electrochem. Soc. 152 (2005) A104–A113.

[15] Larminie, James and Andrew Dicks . "Fuel Cell Systems Explained". Chichester, England; Hoken, NJ: J. Wiley, 2003. pg.49

[16] U.S. Department of Energy Hydrogen Program, 2009 Mar. http://www1.eere.energy.gov/hydrogenandfuelcells/fuelcells/fc_challenges

[17] D. Andress, S. Das, F. Joseck, and T. D. Nguyen. "Status of advanced light-duty transportation technologies in the US". *T. Energy Policy* vol. 4. 2012. pg. 348-364

[18] Zelenay, P., DOE Fuel Cell Technologies, Webinar, April 25, 2011. http://www1.eere.energy.gov/hydrogenandfuelcells/pdfs/zelenay042511.pdf

[19] Johnson Matthey, March 2011.http://www.platinum.matthey.com/pgm-prices

[20] N. Yousfi-Steiner, P. Mocotéguy, D. Candusso, D. Hissel, J. Power Sources 194 (2009) 130–145.

[21] Q. Yan, H. Toghiani, H. Causey, J. Power Sources 161 (2006) 492–502.

[22] J. Xie, D.L. Wood III, D.M. Wayne, T.A. Zawodzinski, P. Atanassov, R.L. Borup, J. Electrochem. Soc. 152 (2005) A104–A113.

[23] M.A. Danzer, S.J. Wittmann, E.P. Hofer, J. Power Sources 190 (2009) 86–91.

[24] X. Yan, M. Hou, L. Sun, H. Cheng, Y. Hong, D. Liang, Q. Shen, P. Ming, B. Yi, J. Power Sources 163 (2007) 966–970.

[25] S.D. Knights, K.M. Colbow, J. St-Pierre, D.P. Wilkinson, J. Power Sources 127 (2004) 127–134.

[26] Z. Liu, L. Yang, Z. Mao, W. Zhuge, Y. Zhang, L. Wang, J. Power Sources 157 (2006) 166–176.

[27] K. Mitsuda, T. Murahashi, J. Appl. Electrochem. 21 (1991) 524–530.

[28] R.H. Song, C.S. Kim, D.R. Shin, J. Power Sources 86 (2000) 289–293.

[29] A. Taniguchi, T. Akita, K. Yasuda, Y. Miyazaki, Int. J. Hydrogen Energy 33 (2008) 2323–2329.

[30] Fuel Cell Technology. "Fuel Cell: Working Principles".2012. http://www.fuelcelltechnology.info/

[31] J. Lin. “Synthesis and characterization of MWCNTs supported Pt nanocatalyst for proton exchange membrane fuel cells”. 2009

[32] J. Zhang, H. Wang, D.P. Wilkinson, D. Song, J. Shen. Z. Liu, “Model for the contamination of fuel cell anode catalyst in the presence of fuel stream impurities”. J. Power sources, vol. 147, pp. 58-71, 2005.

[33] M.V. Williams, E. Begg, L. Bonville, H. Russell Kunz, and J.M. Fenton. “Characterization of Gas Diffusion Layers for PEMFC”. Journal of The Electrochemical Societ,. Vol.151 (8), pp. A1173-A1180, 2004.

[34] M. Burst, M. Walker, D. Bethell, D.J. Schiffrin and R. Whyman. “Synthesis of thiol-derivatised gold nanoparticles in a two-phase liquid-liquid system”. J. Chem. Soc., Chem. Communication, pp. 801-802, 1994.

[35] P.C. Hiemenz and R. Rajagopalan. “Principles of colloid and surface chemistry”. New York, Dekker. 1997.

[36] M.F. Mathias, J. Roth, J. Flemming and W. Lehnert. “Handbook of Fuel Cell-Fundamentals, Technology and Applications: Diffusion media materials and characterization”. New York: John Wiley and Sons. Vol. 3, pp. 517-537, 2003.

[37] J.F. Lin, V. Kamavaram, A.M. Kannan, “Synthesis and characterization of CNT supported Pt nanocatalyst for PEMFC,” *Journal of Power Sources*, Vol. 195, Issue 2, 15 January 2010, pp. 466-470.

[38] J.F. Lin, C.W. Mason, A. Adame, X. Liu, X.H. Peng, and A.M.Kannan, “Synthesis of Pt nanocatalyst with micelle-encapsulated multi-walled carbon nanotubes as support for proton exchange membrane fuel cells,” *Electrochimica Acta*, Vol. 55, Issue 22, 1 September 2010, Pages 6496-6500.

[39] J.F. Lin, A. Adame, A.M. Kannan, “Development of durable platinum nanocatalyst on carbon nanotubes for PEMFCs,” *J. Electrochem. Soc.* 157, B846-B851, 2010

[40] T. Yalcına, A. Alemdar , O¨ .I. Ece, N. Gungor. "The viscosity and zeta potential of bentonite dispersions in presence of anionic surfactants"

[41] J. Zhang, L. Gao, "Dispersion of multiwall carbon nanotubes by sodium dodecyl sulfate for preparation of modified electrodes toward detecting hydrogen peroxide," *Materials Letters*, Vol. 61, Issue 17, July 2007, pp. 3571-3574.

[42] C.L. Lee, Y.C. Ju, P.T. Chou, Y.C. Huang, L.C. Kuo, J.C. Oung, "Preparation of Pt nanoparticles on carbon nanotubes and graphite nanofibers via self-regulated reduction of surfactants and their application as electrochemical catalyst, *Electrochemistry Communications*, vol. 7 (2005), pp. 453-458.

[43] A. Ulman, "Formation and structure of self-assembled monolayers," *Chem. Rev*. 1996, 96, pp. 1533-1554.

[44] *Ammonium lauryl sulfate chemical structure*. http://sci-toys.com/ingredients/ammonium_lauryl_sulfate.html.

[45] Joshi, Mohit."Buckyballs-can-be-used-keep-water-pipes-clear-clogging " 2009. http://topnews.in/buckyballs-can-be-used-keep-water-pipes-clear-clogging-2135791

[46] Kroto HW, Heath JR, O'Brien SC, Curl RF, Smalley RE. C60: buckminsterfullerene. *Nature*, 1985; 318:162-3

[47] Davis, Bonnie. *Nanotube Therapy Takes Aim At Breast Cancer Stem Cells*.2012 Feb. http://en.wikipedia.org/wiki/File:Multi-walled_Carbon_Nanotube.png

[48] A.Adam, E. Yli-Rantala, C.-H. Liu, X.-H. Peng, P. Koski, L. Cindrella, P. Kauranen, P.M. Wilde, and A.M. Kannan. "Characterization techniques for gas diffusion layers for proton exchange membrane fuel cells- A review". Journal of Power Sources (2012).

[49] D.C. Graham, *Chem. Rev*., **41** (1947) 441.

[50] R. Parsons, *Modern Aspects of Electrochemistry*, Vol. 1, 1954, p. 103.

[51] P. Delahay, *Double Layer and Electrode Kinetics*, Wiley-Interscience, New York, 1965.

[52] D.M. Mohilner in *Electroanalytical Chemistry*, A.J. Bard, Ed., Dekker, New York, 1966, p 241.

[53] B. Breyer and H.H. Bauer, *Alternating Current Polarography and Tensammetry*, *Chemical Analysis Series*, P.J. Elving and I.M. Kolthoff, Eds., Wiley-Interscience, New York, 1963.

[54] D.E. Smith in *Electroanalytical Chemistry*, A.J. Bard, Ed., Dekker, New York, Vol. 1, 1966, p.1.

[55] A.M. Bond, *Modern Polarographic Techniques in Analytical Chemistry*, Dekker, New York.

[56] Andrzej Lasia. "Electrochemical Impedance Spectroscopy and its Applications" 1999. New York. Vol. 32. p. 143-248.

[57] A.M. Kannan, L. Cindrella, L. Munukutla, Electrochim. Acta 53 (2008) 2416.

[58] A.M. Kannan, L. Munukutla. "Carbon nanochain and carbon nano-fibers based gas diffusion layers for proton exchange membrane fuel cells". J. Power Sources 167 (2007) 330.

[59] X.L. Wang, H.M. Zhang, J.L. Zhang, H.F. Xu, and B.L. Yi. " A bi-functional microporous layer with composite carbon black for PEM fuel cells," *J. Power Sources*, vol, 162, pp.474-479, 2006.

[60] Y.H. Lai, P.A. Rapaport, C. Ji and V. Kumar, "Channel intrusion of gas diffusion media and the effect on fuel cell performance.

[61] E. Antolini, A. Pozio, L. Giorgi, E. Passalacqua, "Morphological characteristics of carbon/polytetraflouroethylene films deposited on porous carbon support, "*J. Materials Sci*.,vol. 33, pp. 1837-1843, 1998.

[62] X. Yuan, H. Wang, J.C. Sun, J. Zhang, "AC impedance technique in PEM fuel cell diagnosis--- A review, " *Int. J. Hydrogen Energy*, vol. 32, pp. 4365- 4380, 2007.

[63] J.F. Lin. Nano-enabled Catalyst for High Power Proton Exchange Membrane Fuel Cells. 2010.

[64] X.L. Wang, H.M. Zhang, J.L. Zhang, H.F. Xu, and B.L. Yi. " A bi-functional micro-porous layer with composite carbon black for PEM fuel cells," J. Power Sources, vol. 162, pp. 474-479, 2006.

[65] Y. H. Lai, P. A. Rappaport, C. Ji, and V. Kumar, "Channel intrusion of gas diffusion media and the effect on fuel cell performance, J. Power Sources, vol. 184, pp. 120-128, 2008.

[66] E. Antolini, A. Pozio, L. Giorgi, E. Passalacqua, "Morphological characteristics of carbon/polytetraflouroethylene films deposited on porous carbon support," *J. Materials*

[67] X. Yuan, H. Wang, J.C. Sun, J. Zhang, "AC impedance technique in PEM fuel cell diagnosis--- A review, " *Int. J. Hydrogen Energy*, vol. 32, pp. 4365- 4380, 2007.

[68] Springer TE, Zawodzinski TA,Wilson MS, Gottesfeld S. "Characterization of polymer electrolyte fuel cells using AC impedance spectroscopy". J. Electrochem Soc 1996;143(2):587–99.

[69] Bernardi DM, Verbrugge MW." A mathematical model of the solid polymer-electrolyte fuel cell". J Electrochem Soc 1992;139(9):2477–91.

[70] Wilson MS, Valerio JA, Gottesfeld S." Low platinum loading electrodes for polymer electrolyte fuel cells fabricated using thermoplastic ionomers". Electrochim Acta 1995;40(3):355–63.

[71] Jordan LR, Shukla AK, Behrsing R, Avery NR, Muddle BC, Forsyth M. "Diffusion layer parameters influencing optimal fuel cell performance". J. Power Sources 2000;86(1–2):250–4.

[72] Passalacqua E, Squadrito G, Lufrano F, Patti A, Giorgi L."Effects of the diffusion layer characteristics on the performance of polymer electrolyte fuel cell electrodes". J Appl Electrochem 2001;31(4):449–54.

[73] Kong CS, Kim DY, Lee HK, Shul YG, Lee TH."Influence of pore size distribution of diffusion layer on mass-transport problems of proton exchange membrane fuel cells". J Power Sources 2002;108(1–2):185–91.

[74] Fisher A, Jindra J, Wendt H."Porosity and catalyst utilization of thin layer cathodes in air operated PEM-fuel cells". J Appl Electrochem 1998;28(3):277–82.

[75] C.Y. Du, B.R. Wang, X.Q. Cheng, J. Power Sources 187 (2009) 505-508and implied self-humidification of PEMFC

[76] *Electrochemical Impedance Spectroscopy (EIS): A Powerful and Cost-Effective Tool for Fuel Cell Diagnostics. Scriber Associates.* http://www.scriber.com